Atmospheric and Climate Sciences, 2025, 15(1), 42-71
https://www.scirp.org/journal/acs
ISSN Online: 2160-0422
ISSN Print: 2160-0414

Evaluating the Performance of Land Surface Models and Microphysics Schemes on Simulation of an Extreme Rainfall Event in Tanzania Using the Weather Research and Forecasting Model

Daniel Gibson Mwageni[1,2], Shuzhou Wang[1*], Godfrey Thomas Assenga[2]

[1]Key Laboratory of Meteorological Disasters of Ministry of Education, Collaborative Innovation Center on Forecast and Evaluation of Meteorological Disasters, Nanjing University of Information Science and Technology, Nanjing, China
[2]Central Forecasting Office, Tanzania Meteorological Authority, Dodoma, Tanzania
Email: dangib92@gmail.com, *wangsz@nuist.edu.cn

How to cite this paper: Mwageni, D.G., Wang, S.Z. and Assenga, G.T. (2025) Evaluating the Performance of Land Surface Models and Microphysics Schemes on Simulation of an Extreme Rainfall Event in Tanzania Using the Weather Research and Forecasting Model. *Atmospheric and Climate Sciences*, **15**, 42-71.
https://doi.org/10.4236/acs.2025.151003

Received: November 12, 2024
Accepted: December 27, 2024
Published: December 30, 2024

Abstract

Precise and accurate rainfall simulation is essential for Tanzania, where complex topography and diverse climatic influences result in variable precipitation patterns. In this study, the 31st October 2023 to 02nd November 2023 daily observation rainfall was used to assess the performance of 5 land surface models (LSMs) and 7 microphysics schemes (MPs) using the Weather Research and Forecasting (WRF) model. The 35 different simulations were then evaluated using the observation data from the ground stations (OBS) and the gridded satellite (CHIRPS) dataset. It was found that the WSM6 scheme performed better than other MPs even though the performance of the LSMs was dependent on the observation data used. The CLM4 performed better than others when the simulations were compared with OBS whereas the 5 Layer Slab produced the lowest mean absolute error (MAE) and root mean square error (RMSE) values while the Noah-MP and RUC schemes produced the lowest average values of RMSE and MAE respectively when the CHIRPS dataset was used. The difference in performance of land surface models when compared to different sets of observation data was attributed to the fact that each observation dataset had a different number of points over the same area, influencing their performances. Furthermore, it was revealed that the CLM4-WSM6 combination performed better than others in the simulation of this event when it was compared against OBS while the 5 Layer Slab-WSM6 combination performed well when the CHIRPS dataset was used for comparison. This research highlights the critical role of the selection of land surface models and microphysics schemes in forecasting extreme rainfall events and underscores the importance of integrating different observational data for model validation. These findings contribute to improving predictive capabilities for extreme rainfall events in similar climatic regions.

Keywords

WRF Model, Parameterization Scheme, Two-Way Nesting, Pattern Correlation

1. Introduction

Tanzania is an African country situated just south of the Equator. Because its precipitation patterns are highly variable due to complex topography and diverse climatic influences, accurate and precise rainfall simulation and forecasting are critical in this region. This country experiences varied rainfall patterns, influenced by its proximity to large water bodies such as the Indian Ocean, as well as the Inter-Tropical Convergence Zone (ITCZ) and the East African monsoon [1]-[4]. These dynamics result in a bimodal rainfall pattern in the northern regions—characterized by the "long rains" from March to May (MAM) and the "short rains" from October to December (OND) and a unimodal pattern in the southern parts, with rains occurring from November through April [5]. The variability in timing, intensity, and spatial distribution of these rainfall events poses significant challenges for weather forecasting, making it essential to develop accurate prediction models for sectors like agriculture, water resource management, and disaster risk reduction.

The WRF model is widely used for simulating weather events in most parts of the world including Tanzania, but its performance is highly sensitive to the choice of parameterization schemes, particularly LSMs and MPs [6] [7]. These schemes represent crucial interactions between the atmosphere, land surface, and hydrometeors, significantly impacting the model's ability to simulate rainfall dynamics accurately. While many global studies have explored the application of LSMs and MPs within the WRF model [8]-[10], there remains a research gap in understanding how these schemes influence rainfall simulations over Tanzania's diverse landscapes.

Globally, the application of LSMs has been instrumental in improving the representation of land-atmosphere interactions in regional climate and weather models. These models simulate surface processes such as energy and moisture fluxes, which directly affect atmospheric conditions [11] [12]. Studies in various regions have shown that different LSMs can significantly influence rainfall predictions [13] [14]. Similarly, MPs are essential in cloud and precipitation modeling, determining how cloud droplets, ice crystals, and other hydrometeors interact to produce precipitation. Recent studies have emphasized the sensitivity of WRF simulations to these schemes, highlighting their role in improving rainfall prediction accuracy, particularly during extreme weather events [15] [16].

In Tanzania and the broader East African region, there has been growing interest in using regional climate models like WRF to enhance weather forecasting capabilities [17] [18]. However, research on the application and optimization of LSMs in Tanzania is still limited compared to other parts of the world. While some studies have evaluated the impact of MPs on precipitation modeling in East Africa [19], comprehensive assessments of specific combinations of LSMs and MPs for Tanzania remain scarce. This research gap highlights the need for studies that investigate the role of these parameterization options in improving rainfall simulations, especially in regions with complex topography and meteorological conditions. This study selects a typical heavy rainfall event in Tanzania which occurred from 31st October to 2nd November 2023 as the case study. Furthermore, a total of 35 numerical simulations were designed, and the observed data from both the ground stations and satellite data (gridded dataset) were used for evaluation. These numerical simulations consist of a combination of 5 LSMs and 7 MPs which are coupled into the WRF model. These combinations are further evaluated and compared in order to determine which one performed better than the others. This study is expected to provide a basis for improving the short-term rainfall prediction over Tanzania as well as providing a theoretical basis for such events.

2. Experiment Design

2.1. Model Configuration

The Weather Research and Forecast (WRF) Model Version 4.4 was used in simulating the rainfall event. This is a community-based Numeric Weather Prediction (NWP) whose dynamic core solves the non-hydrostatic flux form of the Euler equations [20]. WRF uses the Arakawa C-grid coordinate in 96 horizontal directions and in the vertical direction it uses the terrain following hydrostatic pressure coordinates. This NWP model has two cores, the Advanced Research WRF (ARW) core and the Non-hydrostatic Mesoscale Model (NMM) core. In this study, the ARW core was used.

A two-way nesting approach was used in configuring the model domains. The parent domain (d01) had a horizontal resolution of 9 km (362 × 321) covering the entire East African Community while the horizontal resolution of the inner domain (d02) was 3 km (275 × 262). Domain 2 covers the study area that includes the country of Tanzania (**Figure 1**).

The six hourly, 1° × 1° Final Operational Global Analysis data from the National Centers for Environmental Prediction (downloaded from https://rda.ucar.edu/) were used as the initial and boundary conditions data. Since the study area is located near the Equator, the Mercator projection was adopted for this model with an integral timestep of 27s. This study utilized the ability of the WRF model in various parameterizations of land surface schemes and a total of five (5) LSMs and seven (7) MPs were used totaling 35 simulations. The LSMs used were 5 Layer thermal diffusion (5 Layer Slab), Noah LSM [21], Rapid Update Cycle (RUC) Model LSM [22] [23], Noah-multi parameterization (Noah-MP) LSM [24] [25] and the fourth version of the Community Land Model (CLM4) [26]. And MPs used were the Kessler scheme [27], Lin et al. Scheme (Lin) [28], WRF Single-Moment 5-class (WSM5) [29], WRF Single-Moment 6-class [29], New Thompson Scheme [30], Milbrandt-Yau Double-Moment scheme (Milbrandt) [31] and WRF Double-Moment 6-class (WDM6) [32]. The experiment setup is shown in **Table 1**

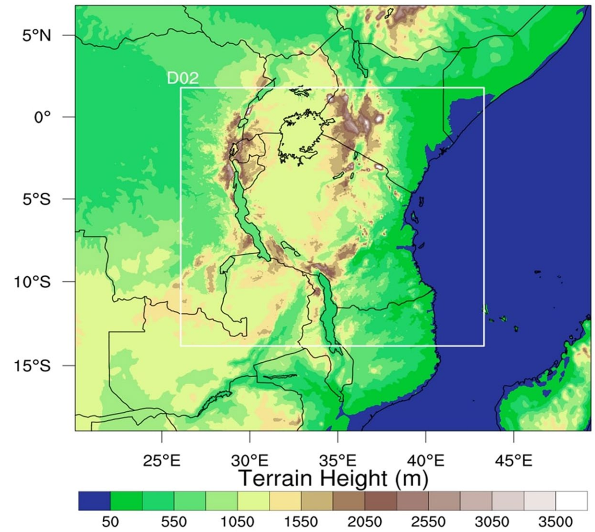

(a)

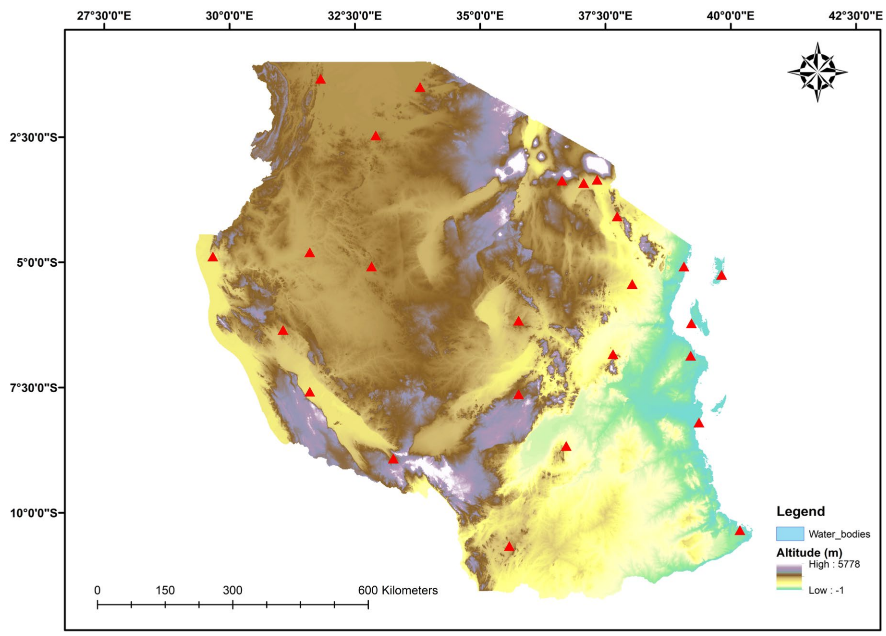

(b)

Figure 1. A map showing (a) the nested domains setup showing the locations of d01 and d02 and (b) the geographical features of the study area as well as its altitude where the red triangle indicates the location of the meteorological stations whose data has been used in this study.

Table 1. The experiment setup of the study. The rows are the MP schemes while the columns are the LSM schemes.

	5 Layer Slab	Noah	RUC	Noah-MP	CLM4
Kessler	SIM 1	SIM 8	SIM 15	SIM 22	SIM 29
Lin	SIM 2	SIM 9	SIM 16	SIM 23	SIM 30
WSM5	SIM 3	SIM 10	SIM 17	SIM 24	SIM 31
WSM6	SIM 4	SIM 11	SIM 18	SIM 25	SIM 32
Thompson	SIM 5	SIM 12	SIM 19	SIM 26	SIM 33
Milbrandt	SIM 6	SIM 13	SIM 20	SIM 27	SIM 34
WDSM6	SIM 7	SIM 14	SIM 21	SIM 28	SIM 35

Additionally, other physics settings used in the simulations are RRTM longwave Radiation Scheme [33], the Dudhia Shortwave Radiation Scheme [34], the Asymmetrical Convective Model version 2 (ACM2) [35] as the Planetary Boundary Layer scheme and the cumulus scheme used was the Grell–Freitas scheme [36]. All these settings were applied to both the outer and inner domains. The simulations were run for 108 hours starting from 1800UTC 30/10/2023 to 0600UTC 04/11/2023 with a spin-up period of 6 hours was used for each simulation.

2.2. Data

The information from the ground meteorological stations was obtained from the Tanzanian Meteorological Authority (TMA). TMA is the authoritative body charged with overseeing all of the meteorological operations within Tanzania, from meteorological data acquisition and distribution to weather forecasts, climate prediction as well as meteorological research (https://www.meteo.go.tz/). The data obtained from TMA was the 2023 daily rainfall from all of the 25 stations currently operational in Tanzania. Then the three consecutive days that received the highest amount of rainfall were selected from the data. For clarity, the observation data from the ground meteorological stations will be referred to as OBS henceforth.

As for the gridded satellite data, the Climate Hazards Group InfraRed Precipitation with Station data (CHIRPS) version 2.0 will be used. CHIRPS is a 35+ year quasi-global rainfall data set spanning 50˚S - 50˚N (and all longitudes) and ranging from 1981 to near-present incorporating 0.05˚ resolution satellite imagery, and in-situ station data to create gridded rainfall time series for trend analysis and seasonal drought monitoring [37].

The use of two different datasets is essential because each dataset has its limitations *i.e.* Few stations for OBS brings about the need for high-resolution CHIRPS data while CHIRPS being derived from estimates brings about the need for actual observation values (OBS).

2.3. Methodology

To properly evaluate the performance of the model simulations, statistical methods were employed between the data from WRF output of the innermost domain with the help of Python code and the observation data over the study area in assessing the model performance. For the WRF data, in order to get the stations' representatives to be compared with OBS, the area average of the four surrounding grid points for each station was used. For CHIRPS, it was first regridded to match the WRF's resolution before being used for evaluation.

For statistical evaluation, the following statistical measures were used to find the best-performing LSM and MP combination:

- The Root Mean Square Error (RMSE) measures the average magnitude of the errors between predicted and observed values. As it is sensitive to outliers, it is useful for understanding model accuracy and it was calculated using Equation (1) [38] [39]:

$$RSME = \sqrt{\left(\frac{1}{n}\right)\sum_{p=1}^{n}\left(x_p - y_p\right)^2} \tag{1}$$

- The Mean Absolute Error (MAE) which represents the average absolute difference between predicted and observed values. It provides a straightforward interpretation of model performance without being influenced by outliers. This was calculated using Equation (2) [38] [40]:

$$\text{MAE} = \left(\frac{1}{n}\right)\sum_{p=1}^{n}\left|x_p - y_p\right| \tag{2}$$

- The correlation coefficient (r) which is crucial in validating WRF models as it quantifies the relationship between model forecasts and observations, allowing for the assessment of forecast skill and improvements [41]. The formula used in this study is shown by Equation (3) which was adopted from [42]

$$r = \frac{\frac{1}{n}\sum_{p=1}^{n}\left(x_p - \overline{x}\right)\left(y_p - \overline{y}\right)}{\sqrt{\frac{1}{n}\sum_{p=1}^{n}\left(x_p - \overline{x}\right)^2 * \frac{1}{n}\sum_{p=1}^{n}\left(y_p - \overline{y}\right)^2}} \tag{3}$$

where x_p and y_p are the observation value and forecasted values at point p respectively, $\overline{x}$ and $\overline{y}$ are the observation mean and the forecasted mean respectively and n is the total number of points

The spatial variation of r known as the pattern correlation (PC) will be used in this study whereby for the gridded datasets (WRF and CHIRPS) the 2-dimension data will be flattened to 1 dimension and Equation (3) will be used to calculate PC.

- The Centred Root Mean Square Deviation (RMSD) will be used in order to represent it on the Taylor diagram [43]. This will be calculated using the formula described by Equation (4) which was adopted from [42]

$$\text{RMSD} = \sigma_o^2 + \sigma_m^2 - 2r\sigma_o\sigma_m \tag{4}$$

where σ_o and σ_m are the observation's and model's standard deviation respectively and r is the correlation coefficient.

Visually, the performance of the WRF model when compared to OBS was represented using the scatter plots while the performance when compared to the CHIRPS was represented using the Taylor diagram.

3. Results

3.1. Overview of the Rainfall Event

During the three days of 31st October 2023 and 02nd November 2023, most parts of Tanzania experienced heavy rainfall activity especially the eastern part of the country (exceeding 50 mm per day). Some stations such as Zanzibar (Unguja) station (6.2167˚S, 39.2167˚E) reported a rainfall of 100 mm in 1 day and a total of 161.4 mm in three days while the station at Dar es Salaam International Airport (DIA) (6.887˚S, 39.2˚E) reported daily rainfall of 120.7 mm in one day accumulating 214.2 mm in three days. Most of the other observation stations reported rainfall of above 40 mm per day such as the Arusha station (3.3667˚S, 36.6333˚E), Moshi station (3.35˚S, 37.333˚E), Handeni station (5.4333˚S, 38.0333˚E), Pemba station (5.25˚S, 39.8167˚E), Tanga station (5.08333˚S, 39.0667˚E) and Kilwa Masoko station (8.1967˚S, 39.5˚E) among others, which reported 44.1 mm, 68.7

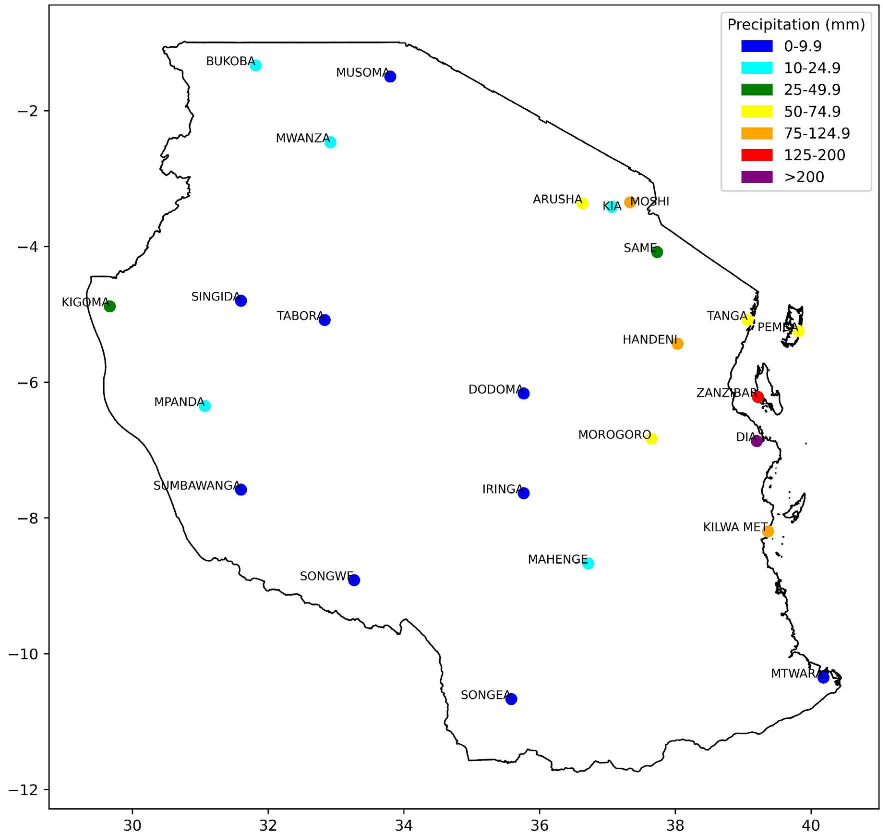

Figure 2. The observed accumulated rainfall from 31st October 2023 to 02nd November 2023 over Tanzania.

mm, 62.8 mm, 43.6 mm, 43.2 mm and 42.1 mm of rainfall per day respectively. It should be noted that these events occurred on three different days for each station and not in one day. Figure 2 shows the three days of accumulated rainfall over Tanzania as observed by the meteorological stations.

3.2. Performance of Different LSMs on the Rainfall Event When Compared with Observation Data from the Ground Station

3.2.1. 5 Layer Slab

The spatial distribution of 5 Layer Slab LSM under different MPs is shown in Figure 3. Most of the MPs captured the centre and its associated amount of extreme

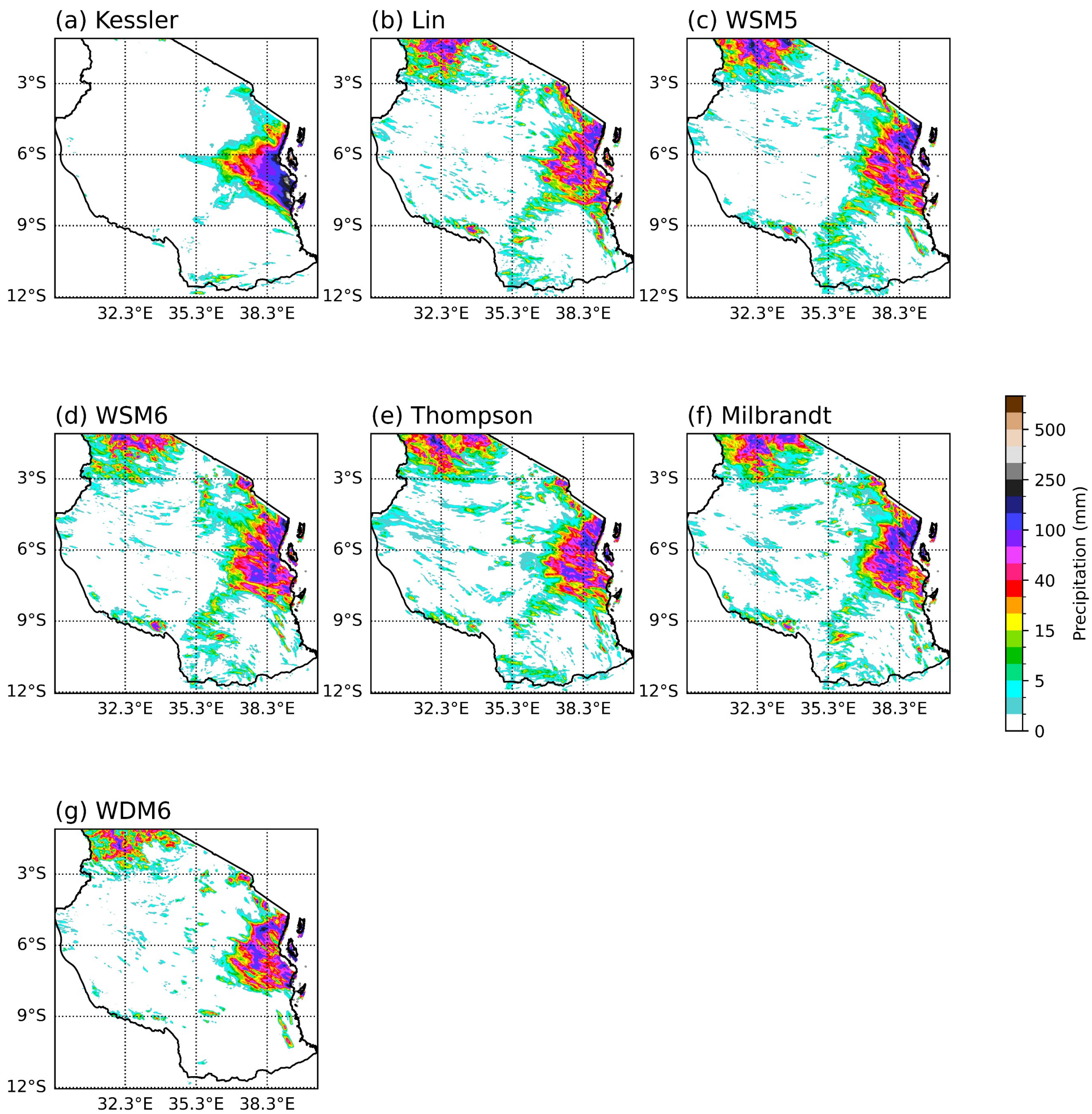

Figure 3. The accumulated rainfall distribution simulated using 5 Layer Slab LSM and (a) Kessler MP, (b) Lin MP, (c) WSM5 MP, (d) WSM6 MP, (e) Thompson MP, (f) Milbrandt MP and (g) WDM6 MP. The simulation started from 0600UTC 31st October 2023 to 0600UTC 03rd November 2023 and the rainfall is in mm.

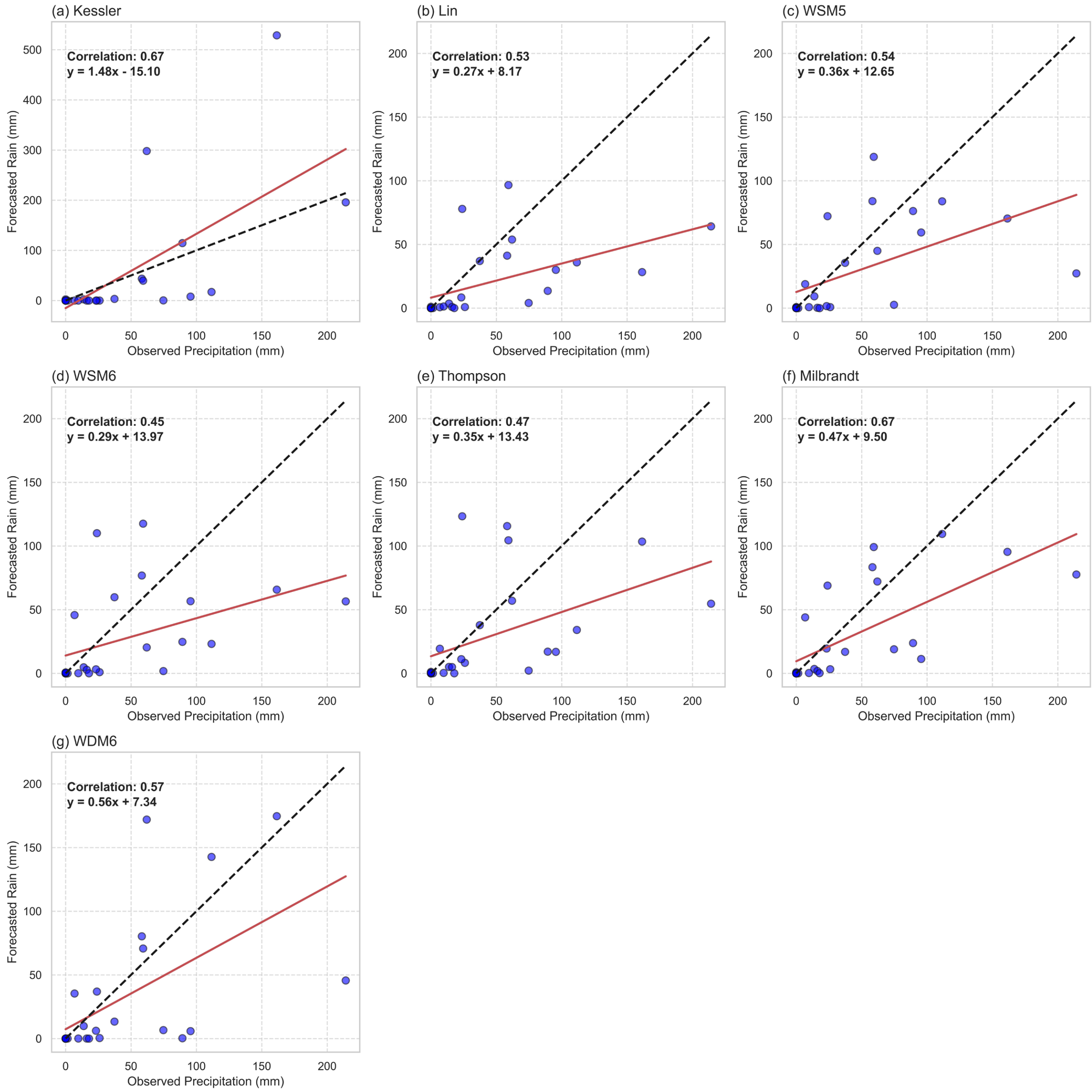

Figure 4. Scatter plots of the observed rainfall from 25 meteorological stations accumulated from 31st October 2023 to 02nd November 2023 against the simulated values under the combination of 5 Layer Slab with the (a) Kessler scheme, (b) Lin scheme, (c) WSM5 scheme, (d) WSM6 scheme, (e) Thompson scheme, (f) Milbrandt scheme and (g) WDM6 scheme. The red line is the line fitted to the y = x line (the black, dotted line). All are in mm.

rainfall rather well. The Kessler scheme concentrated rainfall on the eastern part of the country and some parts of the southern part while drying out the majority of the country. Other schemes distributed rainfall in most parts of the country with high rainfall being in the eastern and northern parts of the country. The maximum amount of rainfall according to the Kessler scheme was above 300 mm located near Dar es Salaam station (DIA). The western and the southern parts had less rainfall amounts compared to the eastern and northern parts. The Lin, WSM5, WSM6, and Milbrandt schemes showed heavy rainfall over the southwestern part of the country depicting amounts greater than 100 mm. While most MPs simulated rainfall activities over the southern part of the country, the WDM6 showed little rainfall activities over that particular region. The Kessler, Lin, Milbrandt, Thompson and WDM6 simulated the maximum amount over the eastern part of the country while WSM5 and WSM6 had maximum values over the northern part.

Both the observation and simulation show heavy precipitation on the eastern coast near Dar es Salaam and Zanzibar islands whereas the central and southern parts of the country were completely dry. To properly evaluate the performance of the simulations, the 3 days accumulated rainfall of all of the 25 observation stations was used. Furthermore, for the simulated data the average of the four grid points surrounding the coordinates of the observation station was used as the model's representative of the corresponding ground station in order to capture the rainfall event more accurately. The PC between the OBS and the simulated values was calculated and shown in **Figure 4**. The results show that most MPs underestimated the rainfall except for the Kessler scheme which overestimated it and in some places the Kessler MP simulated the rainfall of above 500 mm. As for the PC values, both Kessler and Milbrandt schemes had the highest PC value of 0.67 whereas the WSM6 had the lowest correlation value of 0.45.

3.2.2. Noah

The second series of simulations involved the Noah LSM and **Figure 5** shows how it simulated the rainfall event under the combination of 7 different MPs. Like the 5-Layer Slab LSM, the rainfall band appears to be concentrated on the eastern side of the country but unlike the 5-Layer Slab, the high rainfall over the southwestern was not simulated by all MPs. Over the northern parts of the country, the high rainfall coverage also decreased compared to the previous LSM by all but Kessler MP. Most MPs reduced the intensity of rainfall compared to the former LSM with WDM6 being a prime example. Also, the extent of the heavy rainfall band was reduced with most of the inner eastern parts of the country having less rainfall. Still, the majority of the central, western, and southern parts have no rainfall activities within these three days. Thompson scheme simulated the maximum amount over the northern part of the country while the rest of the MPs had maximum values of the Eastern part of the country. Overall, the combination of Noah LSM and the selected MPs showed a reduction of precipitation in most parts of the country.

The scatter plots in **Figure 6** are for the combination of Noah LSM and different MPs. Like under the 5-layer Slab, the Kessler scheme continued to overestimate the rainfall intensity with three stations simulated to have more than 200 mm compared to only one station from the OBS. The rest of the MPs also continued with underestimating the precipitation amount. The WSM6 overestimated the rainfall over Tanga by almost 180 mm and the WDM6 scheme overestimated the rainfall at Pemba station by more than 140 mm. Most MPs performed worse than they did during the simulation run with the combination of 5-layer slab while Kessler, Lin, and Thompson schemes performed better than they did in the previous LSM. Under Noah LSM, the worst-performing MP in terms of PC was the WDM6 which had a very low correlation of 0.22 whereas the Kessler MP had a PC value of 0.72. The Thompson and Lin schemes also performed better and they had a PC value of 0.67 and 0.62 respectively.

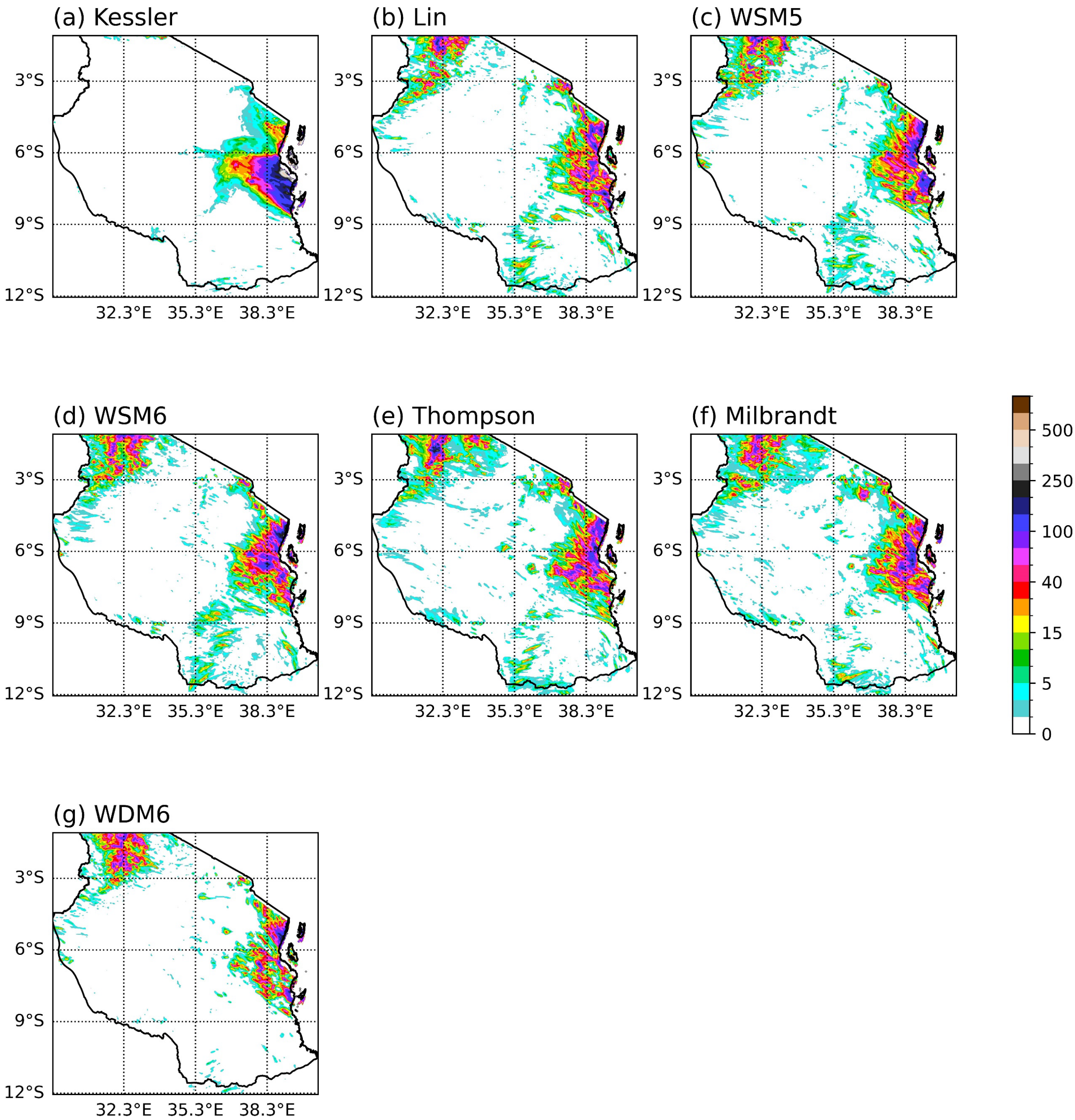

Figure 5. Same as **Figure 3**, but the simulations were for the combinations of Noah LSM and seven different MPs.

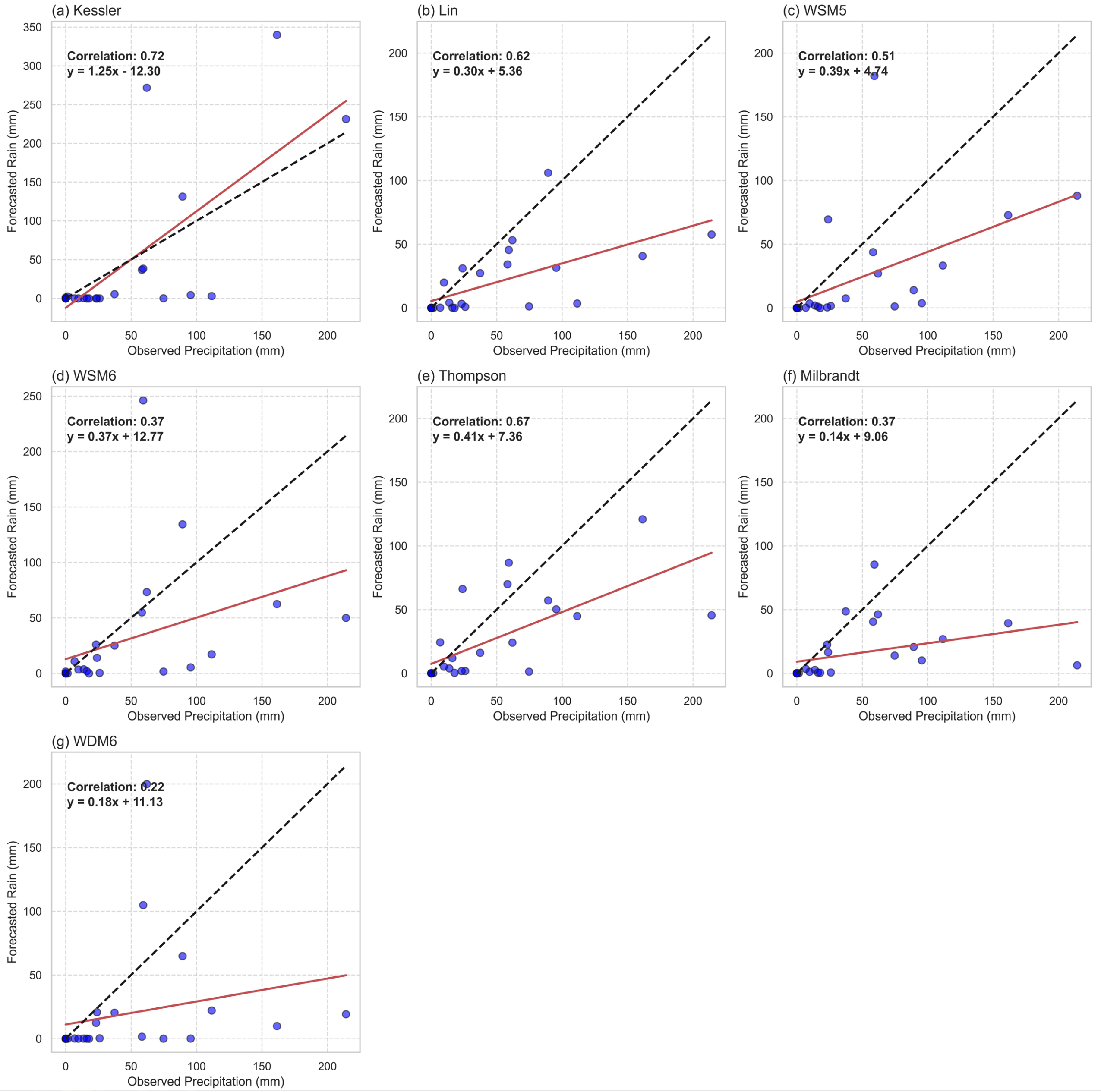

Figure 6. Same as **Figure 4** but for the combination of Noah LSM and the selected MPs.

3.2.3. RUC

The spatial distribution of the simulated rainfall under the combination of RUC LSM and different MPs is shown in Figure 7. Compared to Noah LSM, the RUC LSM produced considerably more precipitation. The Kessler scheme showed some patches of rainfall over northern Tanzania and also over some parts of central and southern Tanzania while still drying most parts of western Tanzania. Also, the coverage of the heavy precipitation band over the eastern coast of Tanzania was shown to have increased compared to the precious LSM for all Microphysics. The Lin, WSM5, WSM6 as well as Milbrandt and WDM6 schemes all showed an increase in rainfall activities over northern Tanzania. Also, the WDM6 scheme showed two precipitation centers over Kigoma region something that other schemes did not detect while drying the majority of the southern part. Similar to the precious LSMs, the Kessler scheme produced the highest amount of rainfall, simulating above 250 mm over Dar es Salaam and Zanzibar areas. Unlike previous LSMs, only the WSM5 and WSM6 MPs had their maximum rainfall in the northern part while the remaining MPs had the maximum values over the eastern part.

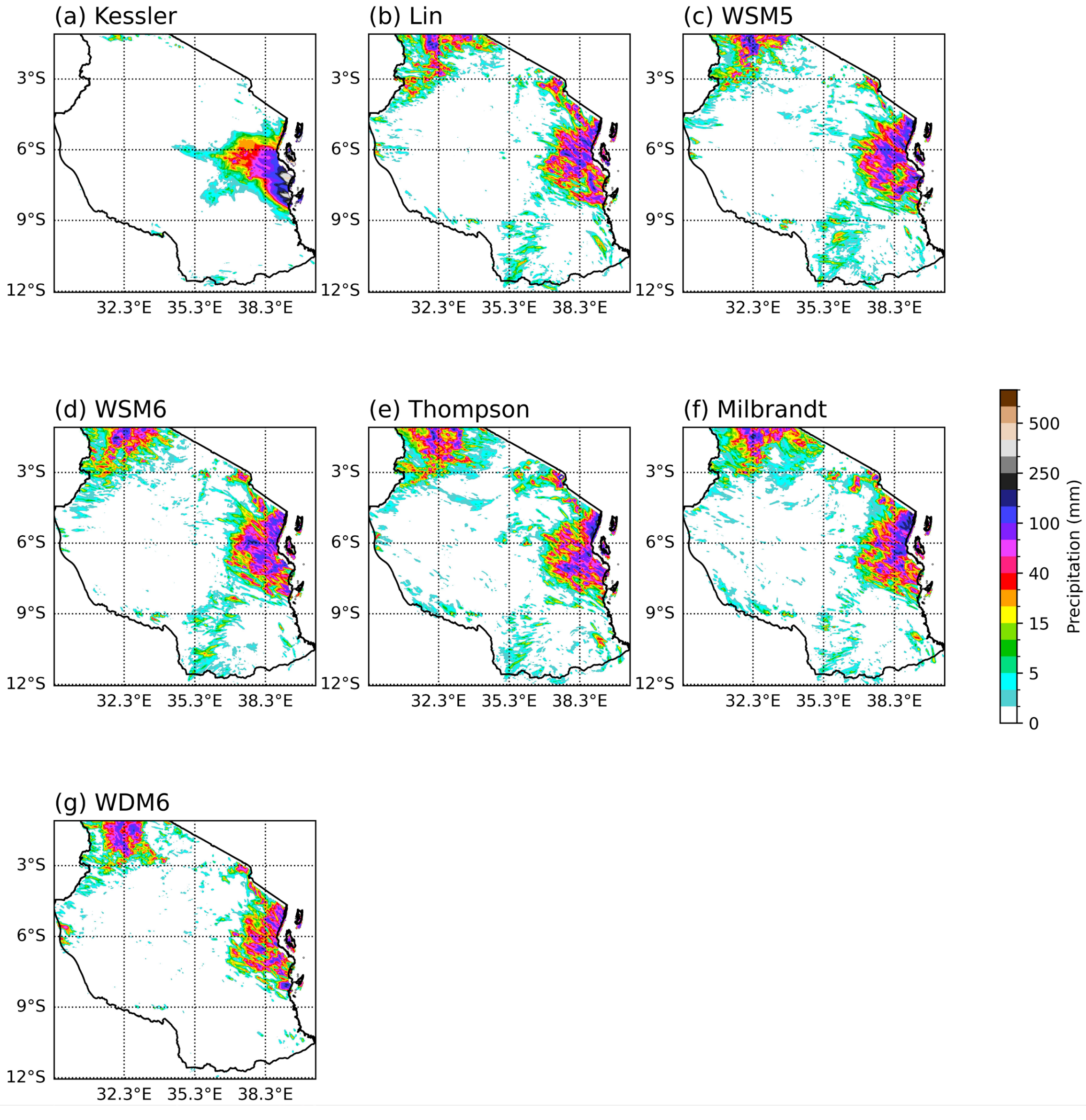

Figure 7. Same as Figure 3, but the simulations were for the combinations of RUC LSM and seven different MPs.

When comparing the simulated and the OBS as seen in Figure 8, the Kessler scheme continues to overestimate the rainfall amount while other MPs continue to underestimate it. Under RUC LSM most MPs performed better than the 5-Layer Slab and Noah LSM except for the Thompson scheme which unexpectedly performed worse. It can also be observed that only the Kessler scheme was able to produce an amount of rainfall greater than 200 mm over DIA while overestimating the amounts over Zanzibar and Kilwa by more than 100 mm and 170 mm respectively. The WSM6 simulated a rainfall value greater than 150 mm at the DIA station and the rest simulated the amount to be less than 100 mm. The Thompson scheme overestimated the rainfall over Tanga by more than 150 mm producing the highest rainfall over that station of all of the MPs. Overall, the scheme with the highest PC under RUC LSM was WSM6 which had a correlation value of 0.83 the highest so far while Kessler, Lin, and WSM5 had PC values of 0.72, 0.65, and 0.64 respectively. The Thompson scheme had the lowest PC of 0.46 with the observed data.

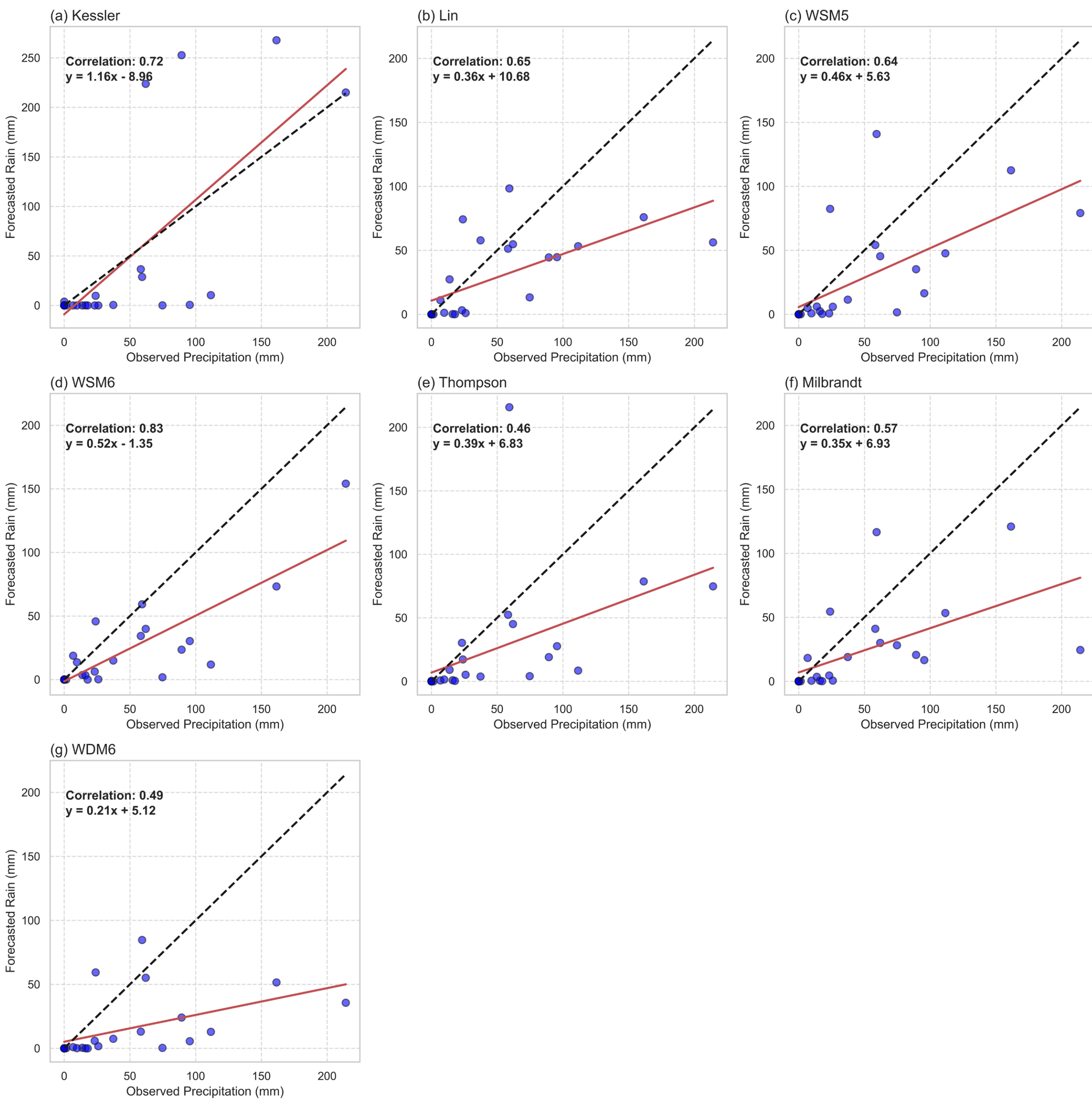

Figure 8. Same as **Figure 4** but for the combination of RUC LSM and the selected MPs.

3.2.4. Noah-MP

Noah-MP is the modified version of the Noah LSM and its spatial distribution for the accumulated rainfall from 31st October 2023 to 02nd November 2023 is shown in Figure 9. Again, it can be observed that this LSM simulated the highest rainfall band over the eastern part of Tanzania with some occurrence of moderate to high amounts of rainfall over the northern part of the country as simulated by all but the Kessler scheme. Thomspon and Milbrandt show the rainfall covering the majority of the country with different intensities while the Kessler scheme simulated rainfall over the eastern coast and some patches over the north, south, and southwestern parts of the country. The highest amount of rainfall can be observed over the regions of Zanzibar and DIA and only the Lin scheme failed to produce any rainfall above 200 mm. On the other hand, the WDM6 scheme showed a

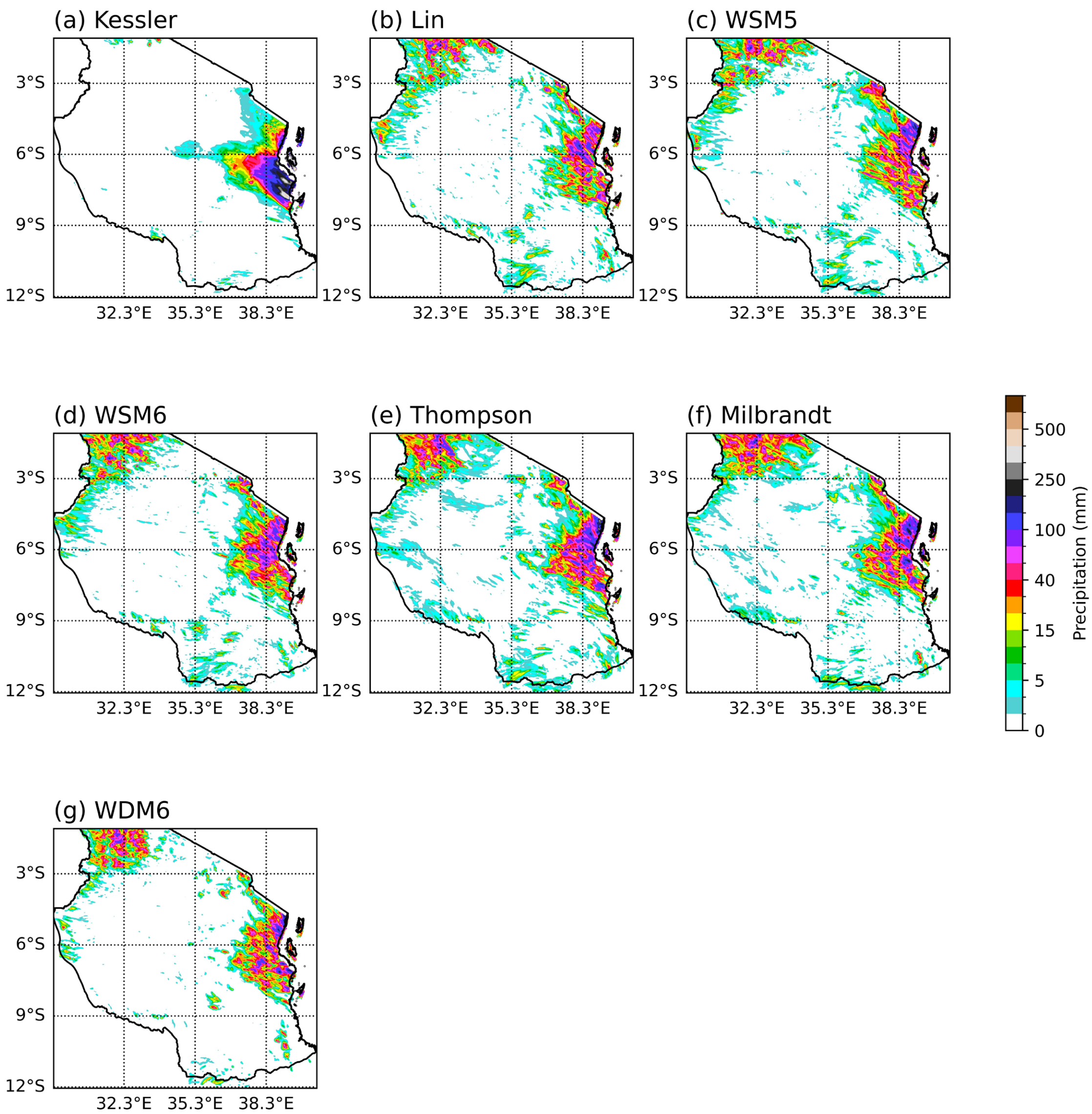

Figure 9. Same as Figure 3, but the simulations were for the combinations of Noah-MP LSM and seven different MPs.

decrease in rainfall in the northern part under Noah-MP compared to the previous LSM. So far, the Noah-MP LSM is the only one whose MPs produced maximum rainfall over the eastern part of the country.

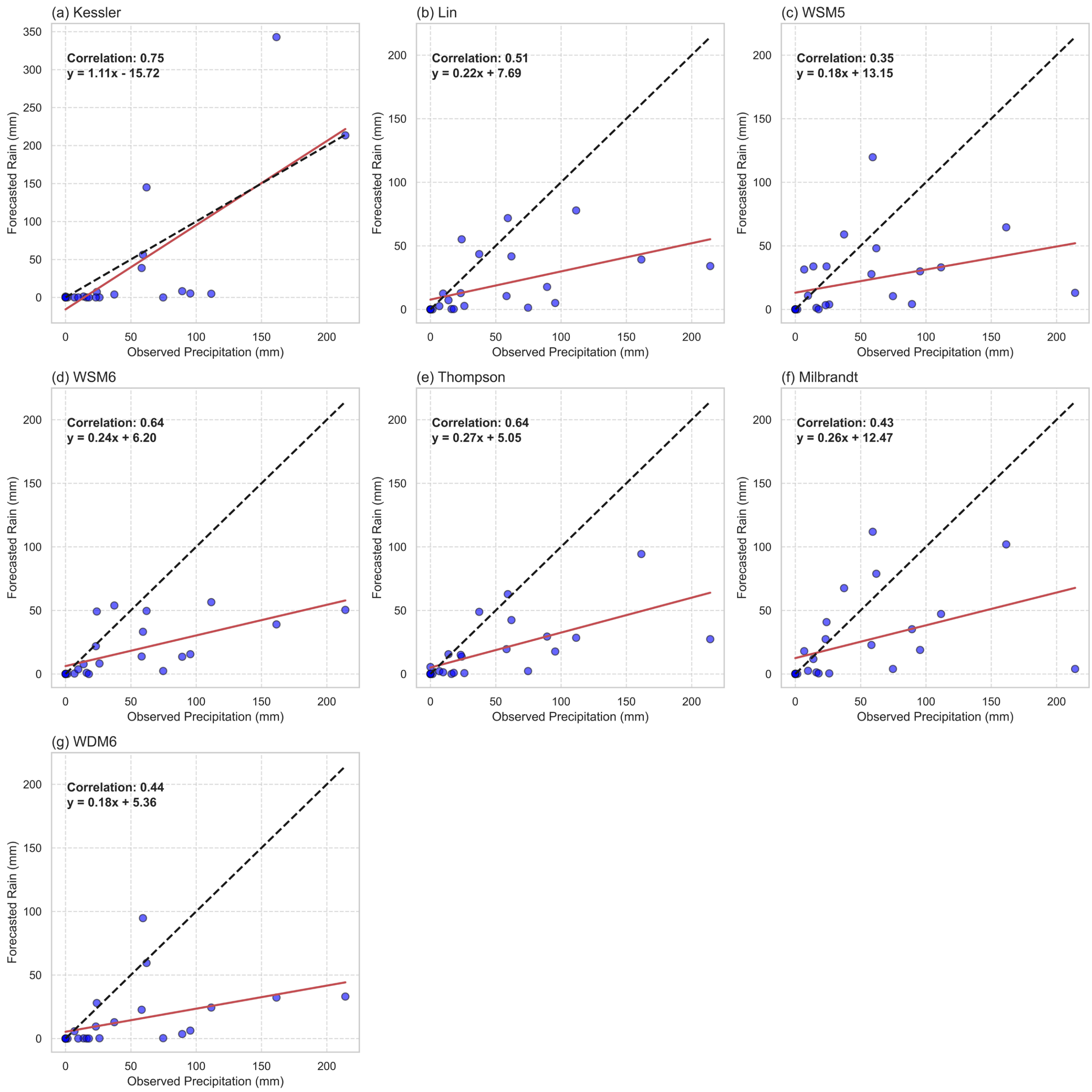

Figure 10. Same as **Figure 4** but for the combination of Noah-MP LSM and the selected MPs.

Figure 10 shows the scatter plots of the simulated against OBS values. On average the Kessler scheme did neither overestimate nor underestimate the rainfall over the given stations while the rest of the MPs continued with their underestimation tendencies similar to the previous LSMs. In terms of spatial distribution all the schemes correctly simulated the highest rainfall band over eastern Tanzania but in terms of the intensity only the Kessler scheme correctly simulated the amount recorded over the DIA station. It simulated a rainfall amount of 213.4 mm which was only 0.8 mm less than the observed value while the rest of the schemes produced rainfall amounts less than 100 mm over the same station contrary to the observation. As observed in the previous LSMs, the Kessler scheme overestimated the rainfall amount over Zanzibar station by approximately 200 mm while the Milbrandt scheme underestimated the rainfall amount over Dar es Salaam by almost 200 mm. In terms of the PC, the highest correlated schemes were the Kessler, the WSM6 and the Thompson schemes which had a value of 0.75, 0.64, and 0.64 respectively while the lowest correlated schemes were the WSM5 and the Milbrandt schemes which had a value of 0.35 and 0.43 respectively.

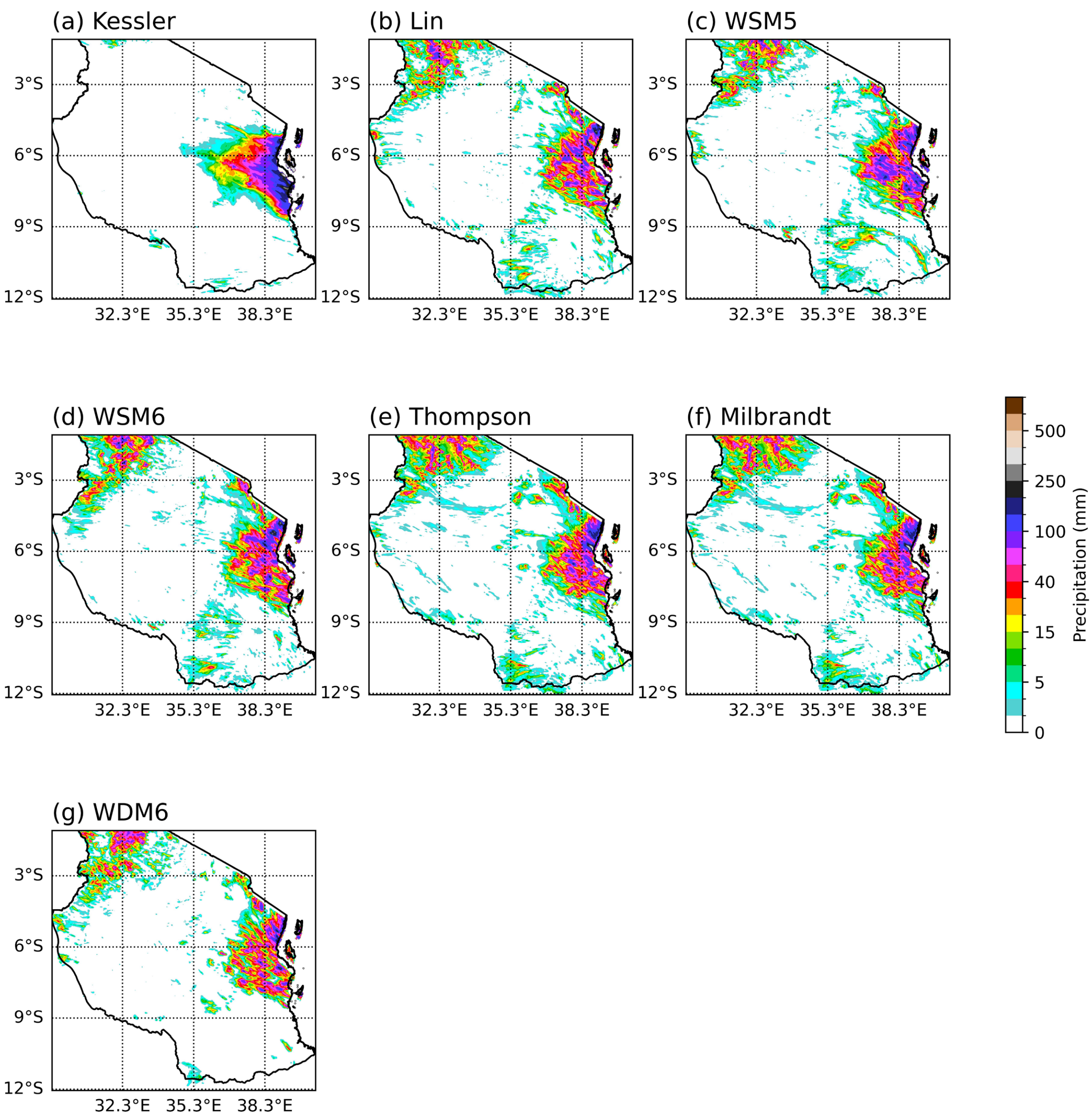

Figure 11. Same as **Figure 3**, but the simulations were for the combinations of CLM4 LSM and seven different MPs.

3.2.5. CLM4

Under the CLM4 LSM, the MPs simulated an increase in high rainfall band coverage as well as its intensity (Figure 11). The Kessler scheme simulated rainfall amount of more than 500 mm over Zanzibar, the highest seen over all the LSM so far. It also continued to dry up the majority of the country except some patches over the north, south, and southwestern of the country. The Lin, WSM5 and WSM6 schemes showed an increase in rainfall activities over the northern part of the country while the Thompson and WDM6 showed a decrease in rainfall activities over the same area compared to the simulations under the previous LSMs.

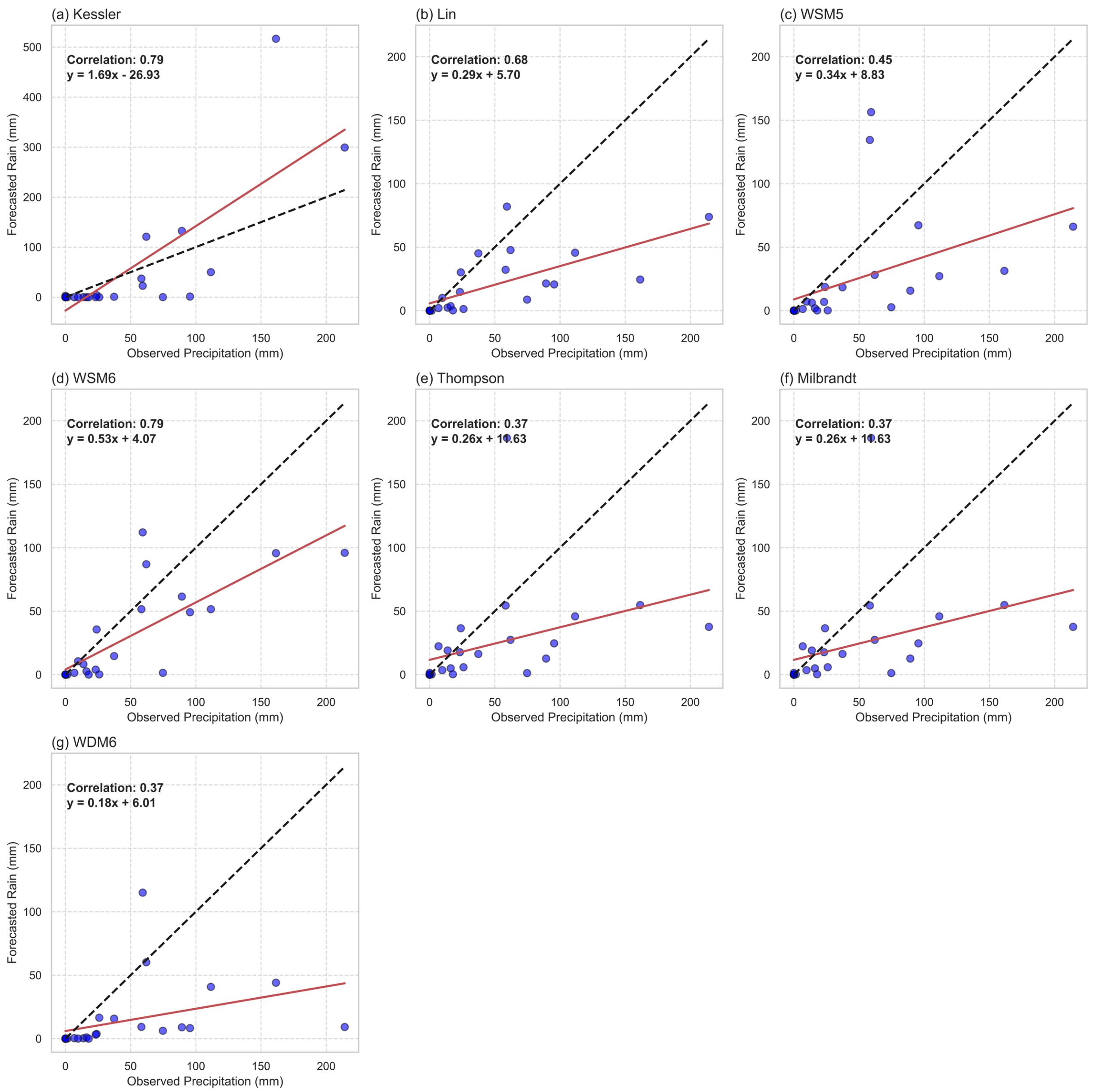

Figure 12. Same as Figure 4 but for the combination of CLM4 LSM and the selected MPs.

The Milbrandt scheme produced almost the same simulation over the majority of the country while the WSM5 increased rainfall activities over the southwestern part of the country. Similar to the previous LSMs, all the MPs under CLM4 simulated their maximum rainfall activities over the eastern parts of the country.

Figure 12 shows the scatter plot of the selected MPs under the CLM4 LSM. The same overestimation and underestimation pattern seen from the previous LSMs can also be seen under the CLM4 LSM. Apart from the Kessler scheme which overestimated the rainfall amount, the rest of the MPs underestimated it. The Kessler scheme seriously overestimated the accumulated rainfall over the DIA and Zanzibar regions by a factor of approximately 100 mm and 350 mm respectively. The WSM5 scheme overestimated the rainfall over the Morogoro and Tanga regions by more than 100 mm while the Thompson and Milbrandt schemes overestimated rainfall over the Tanga region by more than 150 mm. The WSM6 and Kessler schemes had the highest PC values of 0.79 compared to the Lin scheme which had a value of 0.68. The lowest-performing MPs in terms of PC value were the Thompson, Milbrandt and the WDM6 schemes where they all had a correlation value of 0.37.

To further compare and evaluate the simulation using the OBS, the Root Mean Square Error (RSME) and the Mean Absolute Error (MAE) were used. This will enable us to further evaluate which among the tested combinations of LSMs and microphysics schemes did better in simulating the rainfall event.

From Figure 13(a) and Figure 13(b), the combination of the 5-Layer Slab and Kessler scheme produced the highest RMSE of 93.4 mm and it also produced the highest MAE value of 44.42 mm. In terms of the error magnitude, this combination had the worst performance among all other combinations. On the other hand, the error magnitude of CLM4-WSM6 was the smallest among all others with values of 37.9 mm and 23.99 mm respectively showcasing the combination's ability to simulate this rainfall event. A point worth noting is that the WSM6 MP's combination with RUC and CLM4 LSM produced the highest PC as well as the lowest MAE and RMSE respectively.

Those are the results of the rainfall accumulated from the OBS compared to the simulated rainfall produced under the combination of five different LSMs and seven Microphysics schemes. Generally, most of the combinations were able to simulate the highest rainfall center which was over DIA station. Except for the Kessler scheme, most MPs underestimated the rainfall amount under all the LSMs. In terms of the coverage, the Kessler scheme simulated the rainfall over a smaller spatial area compared to other schemes although it produced the highest amount of rainfall leading to the overestimation of the Kessler scheme. It should be noted that the combination of RUC LSM and WSM6 Microphysics produced values that have a very high correlation with the observation while the combination of Noah LSM and WDM6 produced the lowest correlated values with the observation. On the other hand, the combination of Noah-MP and the Kessler scheme produced a very close value to the rainfall observed at the DIA station as it simulated a value of only 0.8 mm less than the observed one. On average, the

WDM6 microphysics performed poorly compared to other MPs and the Noah LSM was the worst-performing LSM as far as PC is considered. Though all of the simulations were able to show the high rainfall band over eastern Tanzania, none was able to accurately simulate an amount close to the one observed over Kigoma station although some LSM schemes were able to simulate the rainfall over that area showcasing the importance of land surface scheme in rainfall simulation over different areas.

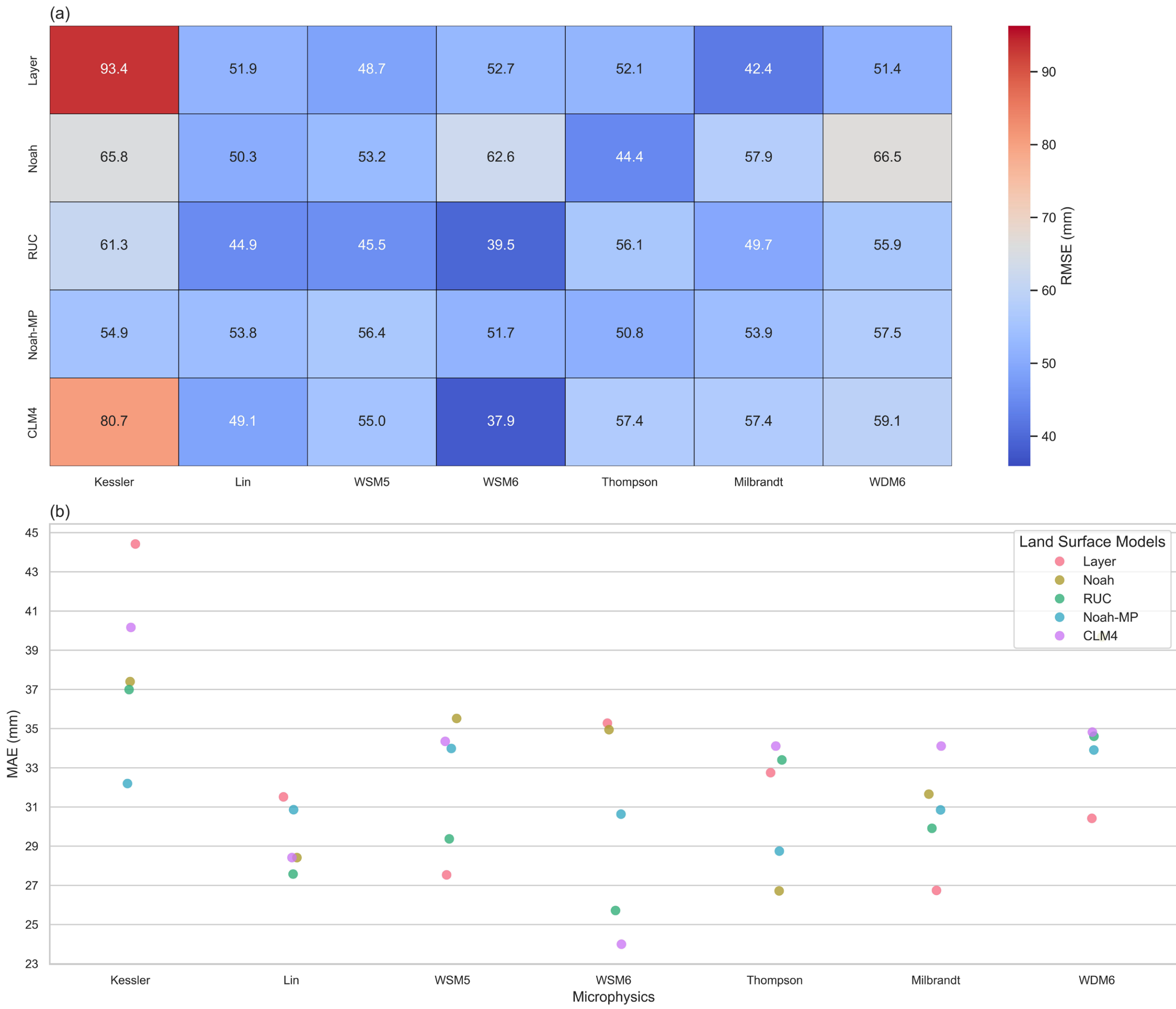

Figure 13. The RMSE in mm (a) and MAE in mm (b) between the accumulated rainfall observed over 25 stations and the simulated values of 3 days accumulated rainfall from 0600UTC 31st October 2023 to 0000UTC 03rd November 2023 for the simulated values. For (b) the pink circle is the 5-Layer Slab LSM, the brown circle represents the Noah LSM, the green circle represents the RUC LSM, the blue circle represents the Noah-MP LSM and the purple circle represents the CLM4 LSM.

3.3. Performance of Different LSMs on the Rainfall Event When Compared with CHIRPS Satellite Dataset

In this section, the performance of different combinations of the WRF model's LSM and MPs was evaluated using the CHIRPS gridded dataset. Similarly, d02 was used in the analysis. The spatial distribution of the rainfall event as recorded by the CHIRPS dataset is shown on **Figure 14**.

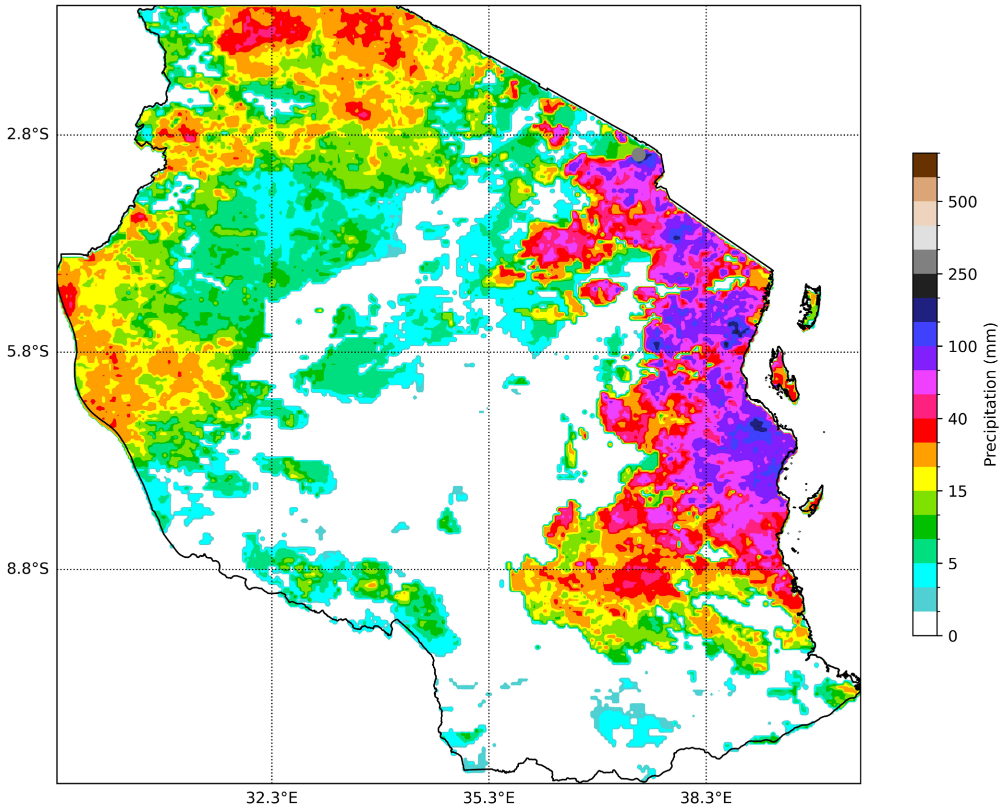

Figure 14. 31st October 2023 to 2nd November 2023 accumulated rainfall distribution over Tanzania using the CHIRPS dataset (in mm). The grey circle represents the location of the maximum rainfall.

Similarly to the observation from the ground station, the CHIRPS dataset also depicts high rainfall activities over the eastern part of the country with the maximum amount being 258.9 mm located at the northeastern highlands of the country at latitude 3.0708˚S and longitude 37.367˚E. The north and western parts of the country experienced moderate rainfall activities same as some of the southern parts of the country. The central part had little to no rainfall activities while the remaining parts of the country had experienced little rainfall. This distribution of rainfall was used to evaluate the performance of the different combinations of LSMs and MPs of the WRF model in terms of its PC (**Figure 15**).

The performances of MPs under the same LSM were almost the same as it is shown by the clustering of the MPs in **Figure 15** except for the Kessler scheme whose high RMSD caused it to not be clustered with other MPs. The highest PC was achieved by the combination of 5 Layer Slab LSM and the WSM6 MP which had a value of 0.578. This PC is not as high as the highest PC when the simulations were evaluated using OBS because the CHIRPS dataset had a lot of rainfall activities, particularly in the northern part and the western part of the country while most WRF simulations and the ground observation data had few scattered rainfall activities over those areas. On the other hand, the combination of Noah LSM and WDM6 MP had the lowest PC of 0.409 compared to other LSMs followed by the combination of 5 RUC and the Kessler scheme which had a PC value of 0.44. This is because these two combinations had fewer rainfall activities over the southern parts of the country as well as the western part of the country (Figure 5(g) and Figure 7(a) respectively). Other combinations had values ranging between 0.451 to 0.560 as shown in Table 2.

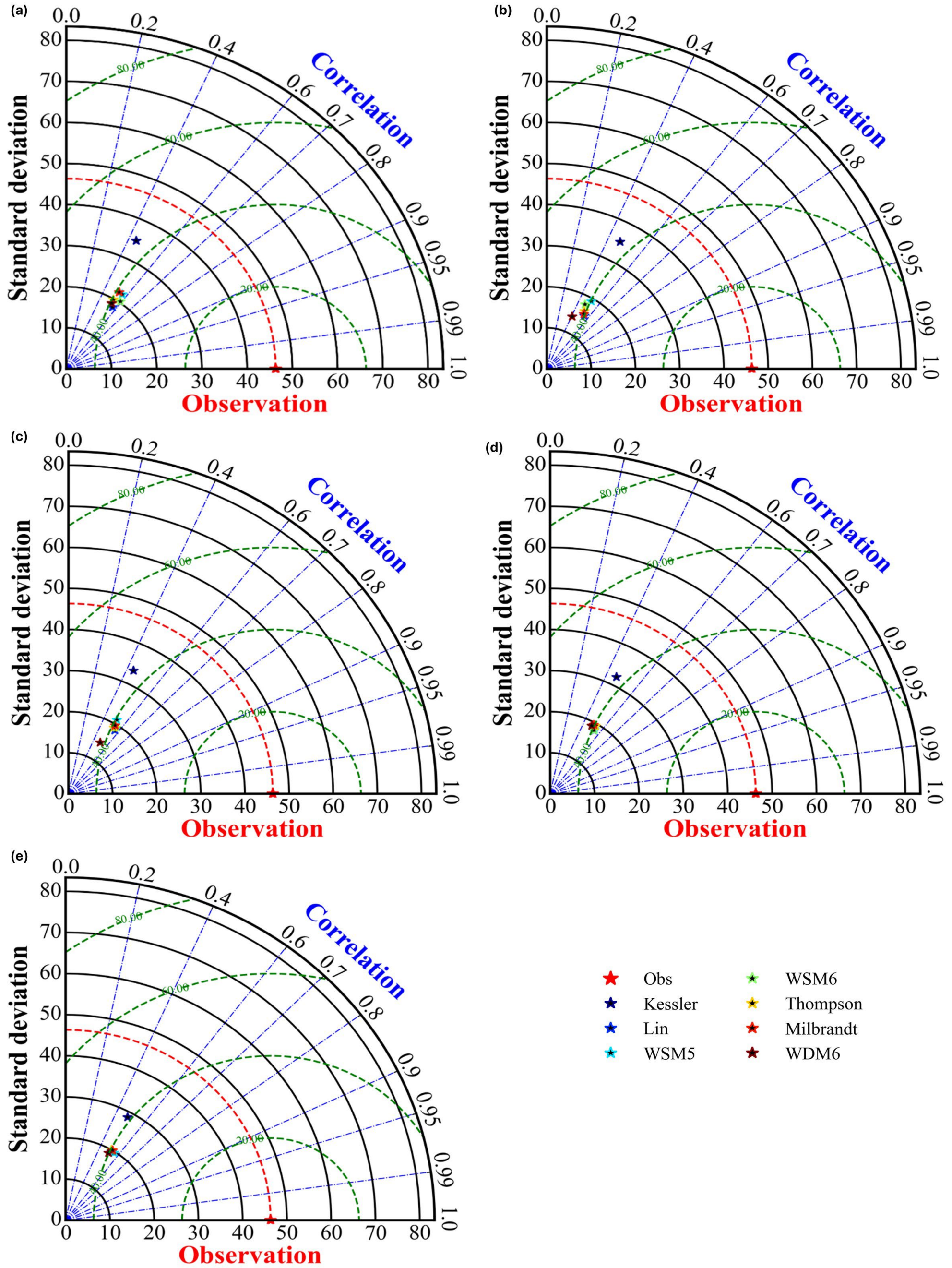

Figure 15. The Taylor diagrams showing the performance of seven MPs under five LSMs which are (a) 5 Layer Slab, (b) Noah, (c) RUC, (d) Noah-MP and (e) CLM4.

Table 2. Pattern Correlation (PC) of different combinations of seven MPs and five LSMs.

	5 Layer Slab	Noah	RUC	Noah-MP	CLM4
Kessler	0.451	0.471	0.441	0.465	0.487
Lin	0.547	0.547	0.561	0.542	0.526
WSM5	0.556	0.521	0.521	0.533	0.554
WSM6	0.578	0.481	0.558	0.541	0.515
Thompson	0.519	0.515	0.538	0.526	0.52
Milbrandt	0.523	0.53	0.536	0.506	0.52
WDM6	0.53	0.409	0.4997	0.49	0.51

On average the 5 Layer Slab had the highest average PC of 0.529 showing that a lot of MPs under this LSM had high PC values while the Noah LSM had the lowest average PC value of 0.496 among all the LSMs. When MPs are compared then the Lin scheme had the average highest PC value of 0.544 while the Kessler scheme had the lowest value of 0.463. The difference between the highest and lowest average values is not big showing that when the simulations of this event are compared with the CHIRPS dataset, they have almost the same performance in terms of PC.

4. Discussion

In this section, the overall performance of each LSM and MP is further discussed to properly evaluate the performance of the different LSMs and MPs combinations' ability to simulate this particular rainfall event. Figure 16 shows the performance of individual MPs and LSMs in terms of RMSE when evaluated using both OBS and CHIRPS datasets.

From Figure 16(a) and Figure 16(c), the Kessler scheme had the highest RMSE which was caused by its overestimation over the eastern part of Tanzania for both OBS and CHIRPS. Especially for the CHIRPS dataset, the Kessler scheme performance was not good considering other MPs had almost the same performance and very low RMSE value compared to the Kessler scheme. On the other hand, the WSM6 had the lowest RMSE value when compared against OBS while the Lin scheme had the lowest median value showing that the combinations of most LSMs and the Lin scheme produced low RMSE values. This is also observed when it is compared using the CHIRPS whereby it had the lowest overall RMSE even though the lowest RMSE value was produced by WSM6. For the LSMs, there was a great variation when they were evaluated using OBS (Figure 16(b)). The CLM4 produced the lowest RMSE value while the RUC LSM had the lowest median value. The two outliers by the 5-Layer Slab and the CLM4 LSM were both produced when they were combined with the Kessler scheme. As for the comparison with the CHIRPS dataset (Figure 16(d)), there were no big variations between the LSMs, all the RMSE values were in the range of 20 mm to 23 mm with the 5-Layer Slab producing the lowest value while the Noah-MP had the lowest median value.

The outliers for all the LSMs were once again produced by the Kessler MP, reflecting its very high RMSE which can be seen in **Figure 16(c)**.

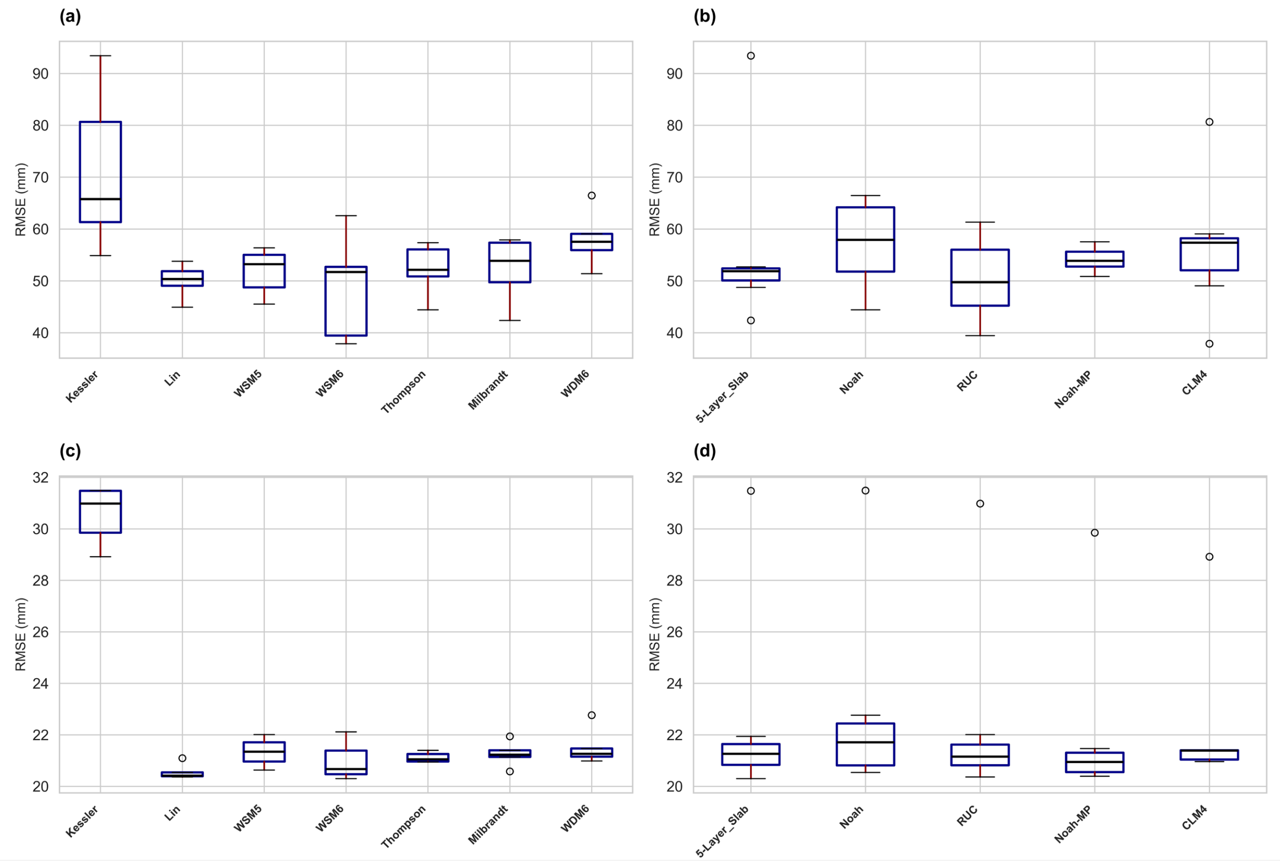

Figure 16. The performance of LSM and MP expressed as RMSE in mm where (a) and (c) are the MPs performance when evaluated against observation data from the ground station and CHIRPS dataset respectively while (b) and (d) show the LSMs performance when evaluated against observation data from the ground station and CHIRPS dataset respectively.

When it comes to MAE (**Figure 17**), the performances of LSMs and MPs were almost the same as those of RMSE. The Kessler scheme had the overall highest MAE values for both OBS (**Figure 17(a)**) and the CHIRPS datasets (**Figure 17(c)**).

The underperforming of the Kessler scheme which was caused by its overestimation of rainfall can be attributed to its linear approach to autoconversion which tends to not account for the variations in the concentration of droplets as well as the size distribution [44] [45] and also it tends to struggle in predicting different autoconversion rates for maritime versus continental clouds [45]. As observed by [46], Kessler's autoconversion rate which increases (decreases) with higher (lower) coefficients or lower (higher) threshold liquid water content tends to impact the precipitation development and the overall accuracy of cloud-related modeling in various atmospheric simulations which could be one of the factors as to why it was outperformed by other MPs. On the other hand, the WSM6 MP had the lowest MAE values for both OBS and the CHIRPS datasets and also the lowest median value highlighting its ability to simulate this particular rainfall event. The good performance of WSM6 could be attributed to its ability to enhance rainfall intensity due to additional hydrometeor categories in high-resolution grids [29]. The WSM6 hydrometeors presentation improves rainfall simulation by incorporating new mass-weighted sedimentation velocities for snow and graupel, enhancing the mixing ratio distribution, and alleviating excessive precipitation issues, leading to more accurate representations of observed precipitation patterns, particularly in short-term rainfall forecasting. Though WSM6 had the best performance in this study, its performance varies based on the meteorological context and the specific event being simulated [47]. For the LSM, the RUC had the lowest MAE value among others while also having the lowest median as well when compared using the CHIRPS dataset but it was second behind CLM4 LSM in terms of the lowest value when it was evaluated using the OBS while it had the lowest median value.

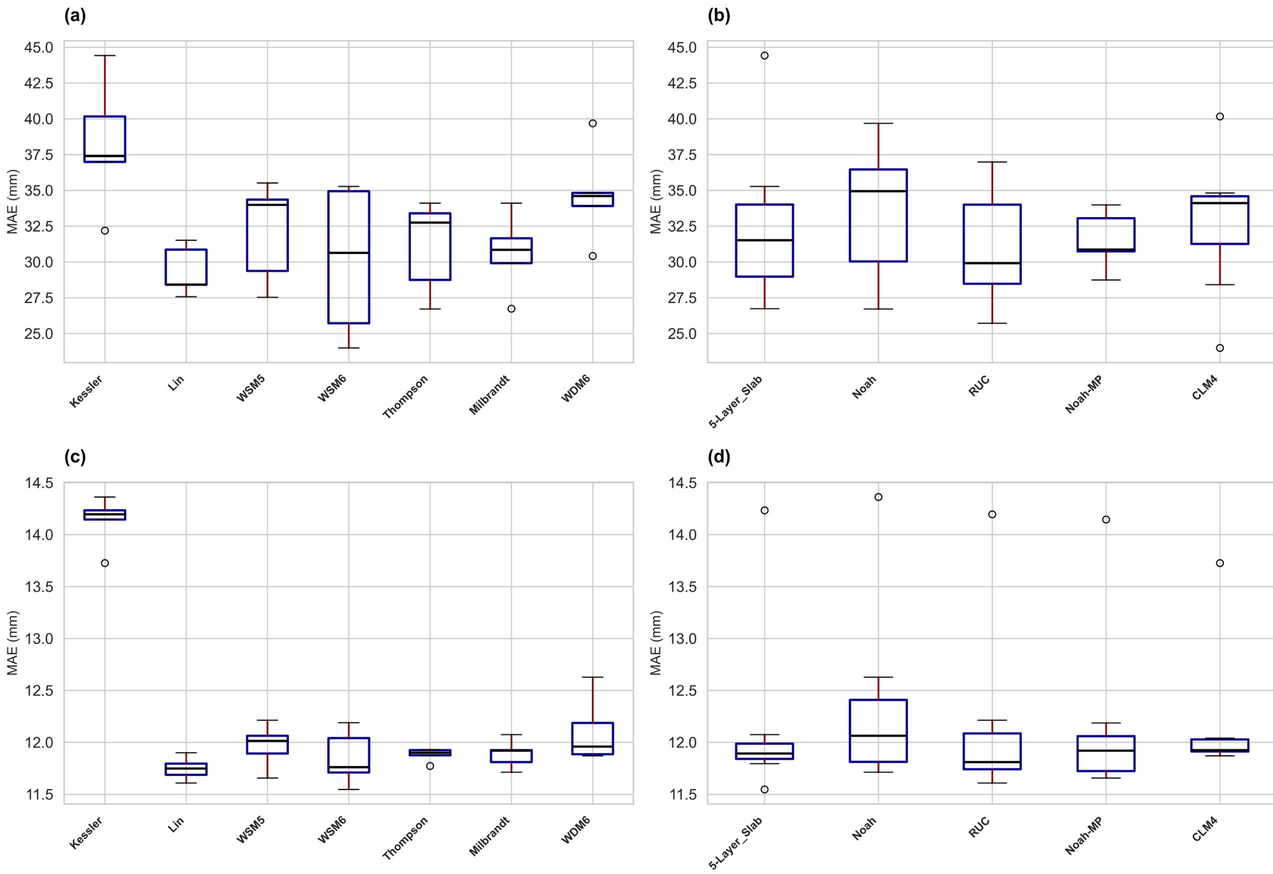

Figure 17. Same as **Figure 16** but for MAE in mm.

Overall, the varying performances of different combinations of LSMs and MPs indicates that the selection of LSM and MP plays a crucial role in accurately simulating extreme weather events [8] [48]-[50]. This is vital in improving the forecasting capabilities in regions prone to such events like Tanzania, which in turn might improve the early warning system regarding weather hazards as better forecasts can lead to better preparedness for extreme events. However, a detailed study under different meteorological conditions as well as a longer period is recommended in order to validate the robustness of these combinations as these results were drawn from a specific rainfall event.

5. Conclusions

This study evaluated the performances of five LSMs and seven MPs in simulating an extreme event in Tanzania using the WRF model. The results revealed significant variability in the accuracy of rainfall simulations among the different model configurations. Notably, the WSM6 demonstrated superior performance when it was paired with CLM4 and 5-Layer Slab when it was evaluated against observation from ground stations as well as gridded satellite data (Chirps) respectively, particularly in terms of RMSE and MAE compared to other configurations.

Furthermore, the findings underscore the importance of utilizing observational data from ground stations and satellite datasets, such as CHIRPS, to validate the output of the model effectively.

Although this study focuses on a single extreme rainfall event, it provides valuable insights into the performance of different LSM and MP combinations. That being said, the results of this study may not generalize to other rainfall events or regions with distinct climatic or topographic conditions in other time periods. Our future work will explore a series of events across different seasons to assess the robustness of the identified configurations. Furthermore, we will focus on refining the model parameters while exploring other physical optimization schemes such as Cumulus, planetary boundary layer as well as radiation schemes all of which can significantly impact rainfall intensity and distribution.

Acknowledgements

This research was jointly supported by the National Natural Science Foundation of China (grant no. 42075156), and the Second Tibetan Plateau Scientific Expedition and Research (STEP) program (2019QZKK0103).

We would like to thank the Tanzanian Meteorological Authority for providing the observation data that were used in this study.

Also, we would like to thank Bliss Jasper who provided the Python script used in plotting the Taylor diagram (https://github.com/Blissful-Jasper/jianpu_record)

Conflicts of Interest

The authors declare no conflicts of interest regarding the publication of this paper.

References

[1] Borhara, K., Pokharel, B., Bean, B., Deng, L. and Wang, S.S. (2020) On Tanzania's Precipitation Climatology, Variability, and Future Projection. *Climate*, **8**, Article No. 34. https://doi.org/10.3390/cli8020034

[2] Francis, J. (2013) Analysis of Rainfall Variations and Trends in Coastal Tanzania.

Western Indian Ocean Journal of Marine Science, **11**, 121-133.

[3] Kijazi, A.L. and Reason, C.J.C. (2005) Relationships between Intraseasonal Rainfall Variability of Coastal Tanzania and Enso. *Theoretical and Applied Climatology*, **82**, 153-176. https://doi.org/10.1007/s00704-005-0129-0

[4] Yonah, I.B., Oteng'I, S.B.B. and Lukorito, C.B. (2006) Assessment of the Growing Season over the Unimodal Rainfall Regime Region of Tanzania Isack Yonah Tanzania Meteor-Ogical Authority (TMA) Assessment of the Growing Season Regime Region of Tanzania over the Unimodal Rainfall. *Tanzania Journal of Agricultural Sciences*, **7**, 16-26.

[5] Kijazi, A. and Reason, C. (2009) Analysis of the 1998 to 2005 Drought over the Northeastern Highlands of Tanzania. *Climate Research*, **38**, 209-223. https://doi.org/10.3354/cr00784

[6] Reddy, B.R., Srinivas, C.V., Shekhar, S.S.R., Baskaran, R. and Venkatraman, B. (2020) Impact of Land Surface Physics in WRF on the Simulation of Sea Breeze Circulation over Southeast Coast of India. *Meteorology and Atmospheric Physics*, **132**, 925-943. https://doi.org/10.1007/s00703-020-00726-5

[7] Deng, C., Chi, Y., Huang, Y., Jiang, C., Su, L., Lin, H., *et al.* (2023) Sensitivity of WRF Multiple Parameterization Schemes to Extreme Precipitation Event over the Poyang Lake Basin of China. *Frontiers in Environmental Science*, **10**, Article 1102864. https://doi.org/10.3389/fenvs.2022.1102864

[8] Di, Z., Zhang, S., Quan, J., Ma, Q., Qin, P. and Li, J. (2023) Performance of Seven Land Surface Schemes in the WRFv4.3 Model for Simulating Precipitation in the Record-Breaking Meiyu Season over the Yangtze-Huaihe River Valley in China. *GeoHealth*, **7**, e2022GH000757. https://doi.org/10.1029/2022gh000757

[9] Teklay, A., Dile, Y.T., Asfaw, D.H., Bayabil, H.K. and Sisay, K. (2019) Impacts of Land Surface Model and Land Use Data on WRF Model Simulations of Rainfall and Temperature over Lake Tana Basin, Ethiopia. *Heliyon*, **5**, e02469. https://doi.org/10.1016/j.heliyon.2019.e02469

[10] Zhou, Z., Du, M., Hu, Y., Kang, Z., Yu, R. and Guo, Y. (2024) An Evaluation and Improvement of Microphysical Parameterization for a Heavy Rainfall Process during the Meiyu Season. *Remote Sensing*, **16**, Article No. 1636. https://doi.org/10.3390/rs16091636

[11] Bakketun, Å., Blyverket, J. and Müller, M. (2023) Using a Reanalysis-Driven Land Surface Model for Initialization of a Numerical Weather Prediction System. *Weather and Forecasting*, **38**, 2155-2168. https://doi.org/10.1175/waf-d-22-0184.1

[12] Henderson, D.S., Otkin, J.A. and Mecikalski, J.R. (2022) Examining the Role of the Land Surface on Convection Using High-Resolution Model Forecasts over the Southeastern United States. *Journal of Geophysical Research: Atmospheres*, **127**, e2022JD036563. https://doi.org/10.1029/2022jd036563

[13] Chao, L., Zhang, K., Wang, S., Gu, Z., Xu, J. and Bao, H. (2022) Assimilation of Surface Soil Moisture Jointly Retrieved by Multiple Microwave Satellites into the WRF-Hydro Model in Ungauged Regions: Towards a Robust Flood Simulation and Forecasting. *Environmental Modelling & Software*, **154**, Article ID: 105421. https://doi.org/10.1016/j.envsoft.2022.105421

[14] Peters-Lidard, C.D., Mocko, D.M., Su, L., Lettenmaier, D.P., Gentine, P. and Barlage, M. (2021) Advances in Land Surface Models and Indicators for Drought Monitoring and Prediction. *Bulletin of the American Meteorological Society*, **102**, E1099-E1122. https://doi.org/10.1175/bams-d-20-0087.1

[15] Nemec, D., Brožková, R. and Van Ginderachter, M. (2024) Developments of Single-

Moment ALARO Microphysics Scheme with Three Prognostic Ice Categories. *Tellus A*: *Dynamic Meteorology and Oceanography*, **76**, 130-147. https://doi.org/10.16993/tellusa.3464

[16] Xu, H., Li, X., Yin, J., Zhou, L., Song, Y. and Hu, T. (2023) Microphysics Affect the Sensitivities of Rainfall to Different Horizontal-Resolution Simulations: Evidence from a Case Study of the Weather Research and Forecasting Model Runs. *Atmospheric Research*, **296**, Article ID: 107022. https://doi.org/10.1016/j.atmosres.2023.107022

[17] Glotfelty, T., Ramírez-Mejía, D., Bowden, J., Ghilardi, A. and West, J.J. (2020) Limitations of WRF Land Surface Models for Simulating Land Use and Land Cover Change in Sub-Saharan Africa and Development of an Improved Model (CLM-AF v. 1.0). *Geoscientific Model Development*, **14**, 3215-3249. https://doi.org/10.5194/gmd-2020-193

[18] Lungo, A., Kim, S., Jiang, M., Cho, G. and Kim, Y. (2020) Sensitivity Study of WRF Simulations over Tanzania for Extreme Events during Wet and Dry Seasons. *Atmosphere*, **11**, Article No. 459. https://doi.org/10.3390/atmos11050459

[19] Pohl, B., Crétat, J. and Camberlin, P. (2011) Testing WRF Capability in Simulating the Atmospheric Water Cycle over Equatorial East Africa. *Climate Dynamics*, **37**, 1357-1379. https://doi.org/10.1007/s00382-011-1024-2

[20] Baki, H., Chinta, S., Balaji, C. and Srinivasan, B. (2021) A Sensitivity Study of WRF Model Microphysics and Cumulus Parameterization Schemes for the Simulation of Tropical Cyclones Using GPM Radar Data. *Journal of Earth System Science*, **130**, Article No. 190. https://doi.org/10.1007/s12040-021-01682-3

[21] Chen, F. and Dudhia, J. (2001) Coupling an Advanced Land Surface-Hydrology Model with the Penn State-NCAR MM5 Modeling System. Part I: Model Implementation and Sensitivity. *Monthly Weather Review*, **129**, 569-585. https://doi.org/10.1175/1520-0493(2001)129<0569:caalsh>2.0.co;2

[22] Smirnova, T.G., Brown, J.M. and Benjamin, S.G. (1997) Performance of Different Soil Model Configurations in Simulating Ground Surface Temperature and Surface Fluxes. *Monthly Weather Review*, **125**, 1870-1884. https://doi.org/10.1175/1520-0493(1997)125<1870:podsmc>2.0.co;2

[23] Smirnova, T.G., Brown, J.M., Benjamin, S.G. and Kim, D. (2000) Parameterization of Cold-Season Processes in the MAPS Land-Surface Scheme. *Journal of Geophysical Research*: *Atmospheres*, **105**, 4077-4086. https://doi.org/10.1029/1999jd901047

[24] Niu, G., Yang, Z., Mitchell, K.E., Chen, F., Ek, M.B., Barlage, M., *et al.* (2011) The Community Noah Land Surface Model with Multiparameterization Options (Noah-MP): 1. Model Description and Evaluation with Local-Scale Measurements. *Journal of Geophysical Research*, **116**, D12109. https://doi.org/10.1029/2010jd015139

[25] Yang, Z., Niu, G., Mitchell, K.E., Chen, F., Ek, M.B., Barlage, M., *et al.* (2011) The Community Noah Land Surface Model with Multiparameterization Options (Noah-MP): 2. Evaluation over Global River Basins. *Journal of Geophysical Research*, **116**, D12110. https://doi.org/10.1029/2010jd015140

[26] Oleson, K.W., Lawrence, D.M., Bonan, G.B., Flanner, M.G., Kluzek, E., Lawrence, P.J., *et al.* (2010) Technical Description of version 4.0 of the Community Land Model (CLM). https://doi.org/10.5065/D6FB50WZ

[27] Kessler, E. (1995) On the Continuity and Distribution of Water Substance in Atmospheric Circulations. *Atmospheric Research*, **38**, 109-145. https://doi.org/10.1016/0169-8095(94)00090-z

[28] Lin, Y., Farley, R.D. and Orville, H.D. (1983) Bulk Parameterization of the Snow Field

in a Cloud Model. *Journal of Climate and Applied Meteorology*, **22**, 1065-1092. https://doi.org/10.1175/1520-0450(1983)022<1065:bpotsf>2.0.co;2

[29] Hong, S.Y. and Lim, J.O.J. (2006) The WRF Single-Moment 6-Class Microphysics Scheme (WSM6). *Journal of the Korean Meteorological Society*, **42**, 129-151.

[30] Thompson, G., Field, P.R., Rasmussen, R.M. and Hall, W.D. (2008) Explicit Forecasts of Winter Precipitation Using an Improved Bulk Microphysics Scheme. Part II: Implementation of a New Snow Parameterization. *Monthly Weather Review*, **136**, 5095-5115. https://doi.org/10.1175/2008mwr2387.1

[31] Milbrandt, J.A. and Yau, M.K. (2005) A Multimoment Bulk Microphysics Parameterization. Part I: Analysis of the Role of the Spectral Shape Parameter. *Journal of the Atmospheric Sciences*, **62**, 3051-3064. https://doi.org/10.1175/jas3534.1

[32] Lim, K.S. and Hong, S. (2010) Development of an Effective Double-Moment Cloud Microphysics Scheme with Prognostic Cloud Condensation Nuclei (CCN) for Weather and Climate Models. *Monthly Weather Review*, **138**, 1587-1612. https://doi.org/10.1175/2009mwr2968.1

[33] Mlawer, E.J., Taubman, S.J., Brown, P.D., Iacono, M.J. and Clough, S.A. (1997) Radiative Transfer for Inhomogeneous Atmospheres: RRTM, a Validated Correlated-k Model for the Longwave. *Journal of Geophysical Research*: *Atmospheres*, **102**, 16663-16682. https://doi.org/10.1029/97jd00237

[34] Dudhia, J. (1989) Numerical Study of Convection Observed during the Winter Monsoon Experiment Using a Mesoscale Two-Dimensional Model. *Journal of the Atmospheric Sciences*, **46**, 3077-3107. https://doi.org/10.1175/1520-0469(1989)046<3077:nsocod>2.0.co;2

[35] Pleim, J.E. (2007) A Combined Local and Nonlocal Closure Model for the Atmospheric Boundary Layer. Part I: Model Description and Testing. *Journal of Applied Meteorology and Climatology*, **46**, 1383-1395. https://doi.org/10.1175/jam2539.1

[36] Grell, G.A. and Freitas, S.R. (2014) A Scale and Aerosol Aware Stochastic Convective Parameterization for Weather and Air Quality Modeling. *Atmospheric Chemistry and Physics*, **14**, 5233-5250. https://doi.org/10.5194/acp-14-5233-2014

[37] Funk, C., Peterson, P., Landsfeld, M., Pedreros, D., Verdin, J., Shukla, S., *et al.* (2015) The Climate Hazards Infrared Precipitation with Stations—A New Environmental Record for Monitoring Extremes. *Scientific Data*, **2**, Article No. 150066. https://doi.org/10.1038/sdata.2015.66

[38] Willmott, C. and Matsuura, K. (2005) Advantages of the Mean Absolute Error (MAE) over the Root Mean Square Error (RMSE) in Assessing Average Model Performance. *Climate Research*, **30**, 79-82. https://doi.org/10.3354/cr030079

[39] Chai, T. and Draxler, R.R. (2014) Root Mean Square Error (RMSE) or Mean Absolute Error (MAE)?—Arguments against Avoiding RMSE in the Literature. *Geoscientific Model Development*, **7**, 1247-1250. https://doi.org/10.5194/gmd-7-1247-2014

[40] Pavia, E.G. (2004) The Uncertainty of Climatological Values. *Geophysical Research Letters*, **31**, L14206. https://doi.org/10.1029/2004gl020526

[41] Siegert, S., Bellprat, O., Ménégoz, M., Stephenson, D.B. and Doblas-Reyes, F.J. (2017) Detecting Improvements in Forecast Correlation Skill: Statistical Testing and Power Analysis. *Monthly Weather Review*, **145**, 437-450. https://doi.org/10.1175/mwr-d-16-0037.1

[42] Biswasharma, R., Umakanth, N., Pongener, I., Longkumer, I., Rao, K.M.M., Pawar, S.D., *et al.* (2024) Sensitivity Analysis of Cumulus and Microphysics Schemes in the WRF Model in Simulating Extreme Rainfall Events over the Hilly Terrain of Nagaland.

Atmospheric Research, **304**, Article ID: 107393. https://doi.org/10.1016/j.atmosres.2024.107393

[43] Taylor, K.E. (2001) Summarizing Multiple Aspects of Model Performance in a Single Diagram. *Journal of Geophysical Research*: *Atmospheres*, **106**, 7183-7192. https://doi.org/10.1029/2000jd900719

[44] Liu, Y. and Daum, P.H. (2003) Toward a Unified Formulation of the Kessler-Type Autoconversion Parameterizations. *Thirteenth ARM Science Team Meeting Proceedings*, Broomfield, 31 March-4 April 2003, 1-5.

[45] Ghosh, S. and Jonas, P.R. (1998) On the Application of the Classic Kessler and Berry Schemes in Large Eddy Simulation Models with a Particular Emphasis on Cloud Autoconversion, the Onset Time of Precipitation and Droplet Evaporation. *Annales Geophysicae*, **16**, 628-637. https://doi.org/10.1007/s00585-998-0628-2

[46] Liu, Y. and Daum, P.H. (2004) Parameterization of the Autoconversion Process. Part I: Analytical Formulation of the Kessler-Type Parameterizations. *Journal of the Atmospheric Sciences*, **61**, 1539-1548. https://doi.org/10.1175/1520-0469(2004)061<1539:potapi>2.0.co;2

[47] Chakraborty, T., Pattnaik, S., Jenamani, R.K. and Baisya, H. (2021) Evaluating the Performances of Cloud Microphysical Parameterizations in WRF for the Heavy Rainfall Event of Kerala (2018). *Meteorology and Atmospheric Physics*, **133**, 707-737. https://doi.org/10.1007/s00703-021-00776-3

[48] Sharma, A., Sharma, D., Panda, S.K. and Kumar, A. (2024) Sensitivity Analysis of Different Parameterization Schemes of the Weather Research and Forecasting (WRF) Model to Simulate Heavy Rainfall Events over the Mahi River Basin, India. *Agricultural and Forest Meteorology*, **346**, Article ID: 109885. https://doi.org/10.1016/j.agrformet.2023.109885

[49] Lu, S., Guo, W., Xue, Y., Huang, F. and Ge, J. (2021) Simulation of Summer Climate over Central Asia Shows High Sensitivity to Different Land Surface Schemes in WRF. *Climate Dynamics*, **57**, 2249-2268. https://doi.org/10.1007/s00382-021-05876-9

[50] Köcher, G., Zinner, T. and Knote, C. (2022) Influence of Cloud Microphysics Schemes on Weather Model Predictions of Heavy Precipitation. *Atmospheric Chemistry and Physics*, **23**, 6255-6269. https://doi.org/10.5194/acp-2022-835